WYOMING STATE GEOLOGICAL SURVEY
Thomas A. Drean, Director and State Geologist
Laramie, Wyoming

Interpreting the past, providing for the future

OPEN FILE REPORT 2017-6
Bridger Pass 1:24,000-scale Bedrock Geologic Map

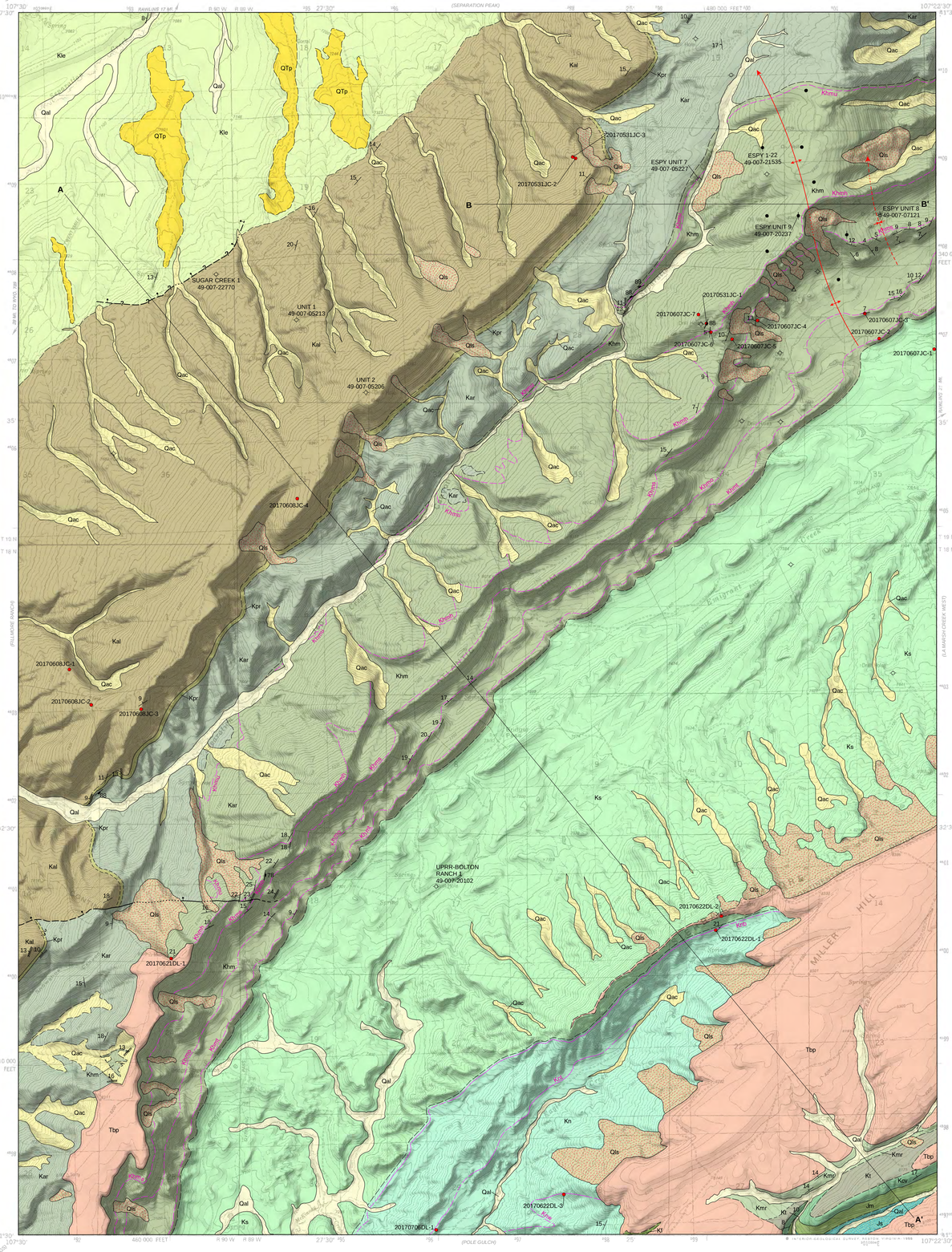

Base map from U.S. Geological Survey 1:24,000-scale topographic map of the Bridger Pass, Wyoming Quadrangle, 1983

Base hillshade derived from United States Elevation Data (NED), 10-meter Digital Elevation Model (DEM), 2008; azimuth 315º, sun angle 45º, vertical exaggeration 1.5

Projection: Universal Transverse Mercator (UTM), zone 13
North American Datum of 1927 (NAD 27)
1,000-meter grid ticks: UTM, zone 13
10,000-foot grid ticks: Wyoming State Plane Coordinate System, east central zone

Wyoming State Geological Survey
P.O. Box 1347 - Laramie, WY 82073-1347
Phone: 307-766-2286 - Fax: 307-766-2605
Email: wsgs-info@wyo.gov

MN
GN
1°37'
9°40'
UTM GRID AND 2017 MAGNETIC NORTH DECLINATION AT CENTER OF SHEET

SCALE 1:24,000
1 0.5 0 1 Mile
1,000 0 1,000 2,000 3,000 4,000 5,000 6,000 7,000 Feet
1 0.5 0 1 Kilometer
CONTOUR INTERVAL 20 FEET
NATIONAL GEODETIC VERTICAL DATUM OF 1929

WYOMING QUADRANGLE LOCATION

Digital cartography by Derek T. Lichtner
Map edited by Suzanne C. Luhr

Prepared in cooperation with and research supported by the U.S. Geological Survey, National Cooperative Geologic Mapping Program, under USGS award number G16AC00199. The views and conclusions contained in this document are those of the authors and should not be interpreted as necessarily representing the official policies, either expressed or implied, of the U.S. Government.

PRELIMINARY GEOLOGIC MAP OF THE BRIDGER PASS QUADRANGLE, CARBON COUNTY, WYOMING

by

Derek T. Lichtner, Jacob D. Carnes, Seth J. Wittke, and Christopher J. Carroll

2017

EXPLANATION

CORRELATION OF MAP UNITS

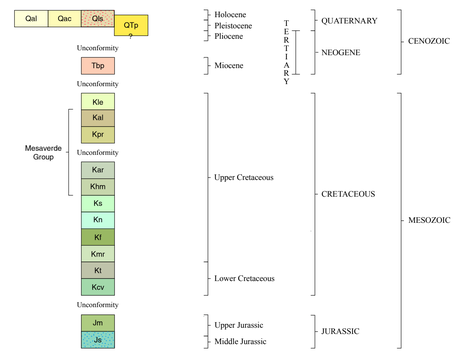

MAP SYMBOLS

Definitions
Certain—Estimated location <25 m (82 ft)
Approximate—Estimated location 25–100 m (82–330 ft)
Inferred—Estimated location >100 m (330 ft)

Formation contact—Continuous where certain, long dash where approximate, short dash where inferred, queried where identity or existence uncertain

Khmt **Key bed**—Continuous where certain, long dash where approximate

Fault—Continuous where certain, long dash where approximate, short dash where inferred, dotted where concealed, queried where identity or existence uncertain, bar and ball on downthrown block of normal fault

Anticline—Continuous where certain, dotted where concealed; arrow on end indicates direction of plunge

Syncline—Short dash where inferred, dotted where concealed; arrow on end indicates direction of plunge

A A' **Line of cross section**

14 **Strike and dip of inclined bedding**

13 **Strike and dip of bedding in cross-bedded rocks**

88 **Strike and dip of joint**

20170531JC-2 **Sample location**—Showing sample name (refer to accompanying report for analyses)

WELLS (Showing API number and drill hole name if projected to cross section or in composite type log)

Active disposal well

Dry hole

Idle gas well

Idle oil well

Producing oil well

REFERENCES

Berry, D.W., 1960, Geology and ground-water resources of the Rawlins area, Carbon County, Wyoming: U.S. Geological Survey Water-Supply Paper 1458, 74 p., 1 pl., scale 1:63,360.

Case, J.C., and Hallberg, L.L., circa 1996, Preliminary landslide map of the Bridger Pass quadrangle, Carbon County, Wyoming (unpublished): Wyoming State Geological Survey, scale 1:24,000.

Finn, T.M., and Johnson, R.C., 2005, Niobrara total petroleum system in the southwestern Wyoming Province, chap. 6 *of* U.S. Geological Survey Southwestern Wyoming Province Assessment Team, comp., Petroleum systems and geologic assessment of oil and gas in the southwestern Wyoming Province, Wyoming, Colorado, and Utah: U.S. Geological Survey Digital Data Series 69-D, 27 p.

Gill, J.R., Merewether, E.A., and Cobban, W.A., 1970, Stratigraphy and nomenclature of some Upper Cretaceous and lower Tertiary rocks in south-central Wyoming: U.S. Geological Survey Professional Paper 667, 53 p.

Haacke, J.E., Barclay, C.S.V., and Hettinger, R.D., 2016, Preliminary geologic mapping of Cretaceous and Tertiary formations in the eastern part of the Little Snake River coal field, Carbon County, Wyoming: U.S. Geological Survey Open-File Report 2016-1170, 9 p.

Hettinger, R.D., Honey, J.G., Ellis, M.S., Barclay, C.S.V., and East, J.A., 2008, Geologic map of Upper Cretaceous and Tertiary strata and coal stratigraphy of the Paleocene Fort Union Formation, Rawlins-Little Snake River area, South-Central Wyoming: U.S. Geological Survey Scientific Investigations Map 3053, 3 sheets, scale 1:100,000.

Kirschbaum, M.A., and Roberts, L.N.R., 2005, Stratigraphic framework of the Cretaceous Mowry Shale, Frontier Formation and adjacent units, southwestern Wyoming Province, Wyoming, Colorado, and Utah, chap. 15 *of* U.S. Geological Survey Southwestern Wyoming Province Assessment Team, comp., Petroleum systems and geologic assessment of oil and gas in the southwestern Wyoming Province, Wyoming, Colorado, and Utah: U.S. Geological Survey Digital Data Series 69-D, 31 p., 4 pls.

Martinsen, O.J., 1994, Evolution of an incised-valley fill, the Pine Ridge Sandstone of southeastern Wyoming, U.S.A.—Systematic sedimentary response to relative sea-level change: Society for Sedimentary Geology (SEPM) Special Publication no. 51, p. 109–128.

Mellere, Donatella, and Steel, R.J., 1995, Facies architecture and sequentiality of nearshore and 'shelf' sandbodies; Haystack Mountains Formation, Wyoming, USA: Sedimentology, v. 42, p. 551–574.

Montagne, John, 1991, Cenozoic history of the Saratoga Valley area, Wyoming and Colorado: Rocky Mountain Geology, v. 29, p. 13–70.

Quillinan, S.A., Worman, B.N., and Rodgers, J.R., 2009, Coalbed natural gas activity in the Atlantic Rim area, Carbon County, Wyoming: Wyoming State Geological Survey Open File Report 09-7, scale 1:100,000.

Roehler, H.W., 1990, Stratigraphy of the Mesaverde Group in the central and eastern Greater Green River Basin, Wyoming, Colorado, and Utah: U.S. Geological Survey Professional Paper 1508, 52 p., 2 pls.

Vincelette, R.R., and Foster, N.H., 1992, Fractured Niobrara of northwestern Colorado, *in* Schmoker, J.W., Coalson, E.B., and Brown, C.A., eds., Geological studies relevant to horizontal drilling—Examples from western North America: Rocky Mountain Association of Geologists Guidebook, p. 227–239.

Vine, J.D., and Prichard, G.E., 1959, Geology and uranium occurrences in the Miller Hill area, Carbon County, Wyoming: U.S. Geological Survey Bulletin 1074-F, p. 201–239.

DISCLAIMERS

Users of this map are cautioned against using the data at scales different from those at which the map was compiled. Using these data at a larger scale will not provide greater accuracy and is a misuse of the data.

The Wyoming State Geological Survey (WSGS) and the State of Wyoming make no representation or warranty, expressed or implied, regarding the use, accuracy, or completeness of the data presented herein, or of a map printed from these data. The act of distribution shall not constitute such a warranty. The WSGS does not guarantee the digital data or any map printed from the data to be free of errors or inaccuracies.

The WSGS and the State of Wyoming disclaim any responsibility or liability for interpretations made from, or any decisions based on, the digital data or printed map. The WSGS and the State of Wyoming retain and do not waive sovereign immunity.

The use of or reference to trademarks, trade names, or other product or company names in this publication is for descriptive or informational purposes only, or is pursuant to licensing agreements between the WSGS or State of Wyoming and software or hardware developers/vendors, and does not imply endorsement of those products by the WSGS or the State of Wyoming.

DESCRIPTION OF MAP UNITS

Cenozoic

Qal **Alluvium (Quaternary)**—Unconsolidated sand, silt, clay, coarse gravels and cobbles, mainly in floodplains and along ephemeral streams. Material locally derived. Thickness less than 8 m (26 ft)

Qac **Alluvium and colluvium, undivided (Quaternary)**—Unconsolidated clay, silt, sand, and gravel derived from local units and deposited in floodplains and along ephemeral streams. Includes slope wash and small alluvial fan deposits that merge with alluvium. Thickness less than 8 m (26 ft)

Qls **Landslide debris (Quaternary)**—Locally derived landslide debris and slumps from unstable slopes, often involving the Miocene Browns Park Formation or Cretaceous Mesaverde Group along the Miller Hill or Atlantic Rim escarpments. Thickness less than 120 m (390 ft)

QTp **Pediment deposits (Quaternary and Tertiary[?])**—Unconsolidated subangular pebble and cobble gravels in a sandy matrix. Locally derived, particularly from sandstones within the Almond Formation and Lewis Shale. Thickness less than 3 m (10 ft)

Tbp **Browns Park Formation (Miocene[?])**—The formation is predominantly gray-yellow, horizontally stratified, flaggy, very fine to medium-grained sandstone. Sandstones locally are altered and may be calcareous or silicified. Unconformably overlies all older formations. Basal conglomerate is approximately 90 m (300 ft) thick; total thickness undetermined. Vine and Prichard (1959) report a thickness of at least 240 m (790 ft) in the Miller Hill area. Conglomerate at base, with interbedded sandstone, tuffaceous sandstone, and mudstone above. Conglomerate is composed predominantly of subrounded white quartzite clasts, with varying amounts of limestone, granitoids, gneiss, and chert in a friable, poorly sorted silt and sand matrix. Boulders may be up to 1 m (3 ft) in diameter. Coarser and finer materials alternate and interfinger. Graded bedding is common

Mesozoic

Kle **Lewis Shale (Upper Cretaceous)**—Poorly exposed gray to dark-gray shale, weathering light yellow-gray to gray-blue, interbedded with occasional thin, very fine grained sandstones that weather yellow-brown. Base is conformable and gradational, and is mapped at the break in slope west of the Atlantic Rim, above the sandstones of the Almond Formation. The Dad Sandstone Member was not observed. Approximately 700 m (2,300 ft) thick

Mesaverde Group (Upper Cretaceous)

Kal **Almond Formation**—Brown-gray, very fine grained sandstone interbedded with gray-brown mudstone, carbonaceous shale, and coal. Trace fossils are common, particularly *Planolites* and *Ophiomorpha*, and increase in frequency upsection. Occasional bivalve fossils are present throughout. Discontinuous coal beds, ranging in thickness from centimeters up to 1.5 m (5 ft), are common within carbonaceous zones. Petrified wood fragments are also common. Rare honeycomb weathering. Outcrops weather in a striped pattern. Base is gradational and conformable. Approximately 300 m (980 ft) thick

Kpr **Pine Ridge Sandstone**—Massive white-gray sandstone, very fine to medium-grained. Exposure quality is highly variable. Occasional trough cross-bedding, with cross sets up to 0.6 m (2 ft) thick and decreasing in thickness upsection. Individual beds fine upwards. Occasional channel scours and clay-pebble lag deposits. Fossils are rare. Honeycomb weathering. Base is unconformable and sharp. Thickness is variable; less than 45 m (150 ft) thick

Kar **Allen Ridge Formation**—Brown-orange shale, mudstone, and siltstone interbedded with very fine grained gray sandstone lenses that weather rust-orange, contrasting sharply with the lighter colored beds of the underlying Haystack Mountains Formation. Sandstones contain wavy bedding and ripple laminations. Iron-oxide concretions are common, and may be as large as 5 cm (2 in) in diameter. Rare thin coals. Outcrops weather in a striped pattern, and are generally poorly exposed. Base is sharp and conformable. Approximately 290 m (950 ft) thick

Khm **Haystack Mountains Formation**—Gray-brown shale interbedded with very fine to fine-grained, coarsening-upward white-gray sandstones. Bivalve fossils throughout. Bioturbation is common, especially at the top of sandstone beds. Rare, very thin coals are present near the top of the formation. The sandstones increase in thickness and prominence upsection. Uppermost sandstones are massive, fine grained, hummocky cross-stratified, arenitic, and upwards of 30 m (98 ft) thick, while the lowermost sandstones are very fine grained and thinly bedded with rare glauconite and lithics. Five sandstone intervals, from youngest to oldest, correlate to measured sections by Roehler (1990) and Mellere and Steele (1995):

- **Khmu** Uppermost unnamed sandstone
- **Khmh** Hatfield sandstones (Hatfield 1 and Hatfield 2)
- **Khms** Seminoe sandstones (Seminoe 1 through Seminoe 4)
- **Khmo** O'Brien Spring Sandstone
- **Khmt** Tapers Ranch Sandstone

Upper contact mapped above Roehler's uppermost unnamed sandstone member; basal contact mapped at base of lowermost sandstone (Tapers Ranch). Base is conformable and gradational. Approximately 380 m (1,200 ft) thick

Ks **Steele Shale (Upper Cretaceous)**—Poorly exposed dark-gray shale with occasional, poorly exposed lenticular beds of gray-brown sandstone that weather yellow-brown. Sandstones are similar to the lowermost sandstones of the Haystack Mountains Formation, and are very fine grained, containing rare glauconite and lithic fragments. Base is conformable and gradational, and mapped above the uppermost calcareous bench in the Niobrara Formation. Approximately 820 m (2,700 ft) thick

Kn **Niobrara Formation and Sage Breaks Shale, undivided (Upper Cretaceous)**—Soft, dark-gray shale interbedded with white-gray calcareous shale and marl containing zones of calcite mineralization. Calcareous shales occur in three discrete zones, which crop out as resistant ledges of hard, brittle shale (Vincelette and Foster, 1992):

- **Knb** Buck Peak bench
- **Knt** Tow Creek bench
- **Knw** Wolf Mountain bench

The complete thickness of the Niobrara Formation was not observed: the formation's lowermost parts are covered by the Miocene Browns Park Formation. The Sage Breaks Shale presumably is also covered. Base is conformable and gradational (Finn and Johnson, 2005). Subsurface data indicate a thickness of approximately 460 m (1,500 ft) for the combined Niobrara-Sage Breaks interval

Kf **Frontier Formation (Upper Cretaceous)**—Interbedded gray-brown sandstone, gray shale, and thin lenticular beds of chert-pebble conglomerate. Base is conformable, although there exist several intra-formation unconformities (Kirschbaum and Roberts, 2005). Exposure is limited to a single stream valley in the southeast part of the quadrangle, and the complete thickness was not observed. Subsurface data indicate a thickness of approximately 170 m (560 ft)

Kmr **Mowry Shale (Upper Cretaceous)**—Organic dark-blue-gray, fissile, siliceous shale that weathers into distinct silver-colored plates, forming bare hillslopes paved with broken chips of shale. Basal contact is conformable. The complete thickness of the Mowry Shale was not observed: the formation's uppermost parts are covered by the Miocene Browns Park Formation. Base is conformable. Vine and Prichard (1959) estimated a thickness of 105 m (340 ft) in the Miller Hill area

Kt **Thermopolis Shale (Lower Cretaceous)**—Poorly exposed dark-gray bioturbated shale interbedded with thin beds of poorly exposed gray, ferruginous sandstone. Forms gentle, vegetated slopes composed of soft, dark soil. Base is conformable. Approximately 40–50 m (130–160 ft) thick

Kcv **Cloverly Formation (Lower Cretaceous)**—Sandstone at top, bentonitic shale throughout, and conglomerate at base. The upper sandstone is fine to coarse grained and white-gray, weathering rusty brown. Individual beds within the sandstone are flaggy, subhorizontal, and approximately 5–15 cm (2–6 in) thick. The bentonitic shale is poorly exposed, often forming a grassy, gently rolling surface littered with sandstone float. The conglomerate contains rounded chert pebbles and occasional smoke-gray quartzite and limestone clasts, and is interbedded with lenses of very fine to coarse-grained, cross-bedded sandstone. Basal contact is unconformable. Approximately 50 m (160 ft) thick

Jm **Morrison Formation (Upper Jurassic)**—Poorly exposed interbedded gray and variegated siltstone with nodular freshwater limestone and thin sandstones. Commonly forms slopes peppered with talus from overlying Cloverly Formation conglomerates and sandstones. Approximately 60 m (200 ft) thick

Js **Sundance Formation (Upper and Middle Jurassic)**—Poorly exposed greenish-gray glauconitic shale and sandstone in the upper part, and slope-forming pale-red and gray siltstone and sandstone in the lower part. The complete thickness was not observed; the lowermost parts are covered by Miocene Browns Park Formation. Vine and Prichard (1959) estimated a thickness of 40 m (130 ft) in the Miller Hill area

NOTICE TO USERS OF INFORMATION FROM THE WYOMING STATE GEOLOGICAL SURVEY

The WSGS encourages the fair use of its material. We request that credit be expressly given to the "Wyoming State Geological Survey" when citing information from this publication. Please contact the WSGS at 307-766-2286, ext. 224, or by email at wsgs-info@wyo.gov if you have questions about citing materials, preparing acknowledgments, or extensive use of this material. We appreciate your cooperation.

Individuals with disabilities who require an alternative form of this publication should contact the WSGS. For the TTY relay operator call 800-877-9975.

For more information about the WSGS or to order publications and maps, go to www.wsgs.wyo.gov, call 307-766-2286, ext. 224, or email wsgs-info@wyo.gov.

NOTICE FOR OPEN FILE REPORTS PUBLISHED BY THE WSGS

Open File Reports are preliminary and usually require additional fieldwork and/or compilation and analysis; they are meant to be a first release of information for public comment and review . The WSGS welcomes any comments, suggestions, and contributions from users of the information.

COMPOSITE TYPE LOG

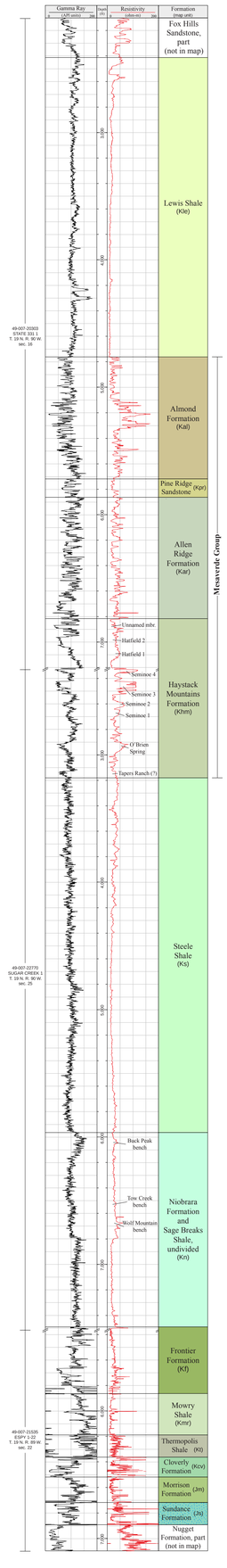

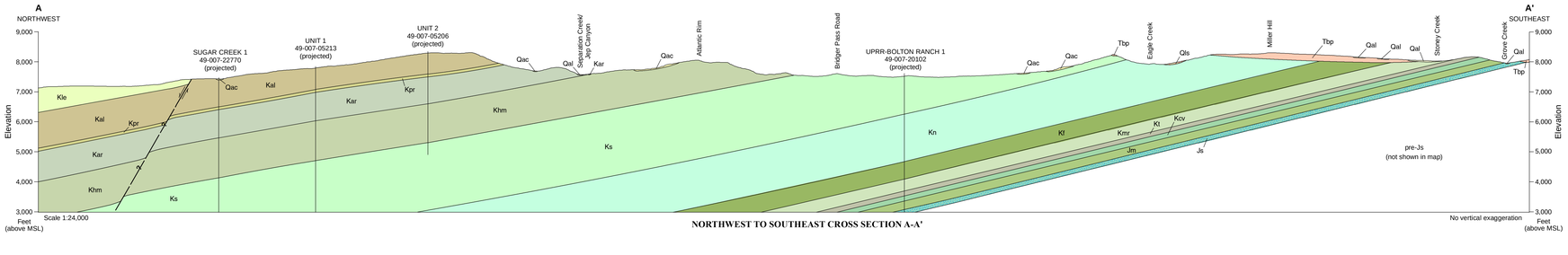

NORTHWEST TO SOUTHEAST CROSS SECTION A–A'

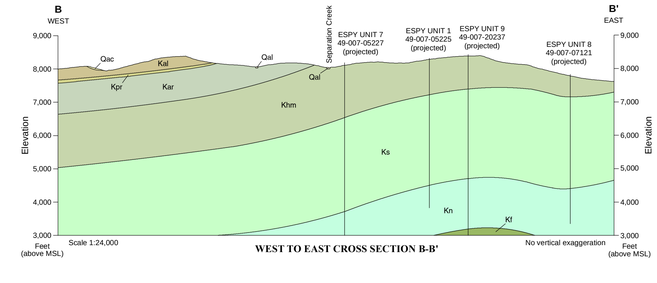

WEST TO EAST CROSS SECTION B–B'

Interpreting the past, providing for the future

Preliminary Geologic Map of the Bridger Pass Quadrangle, Carbon County, Wyoming

By Derek T. Lichtner, Jacob D. Carnes, Seth J. Wittke, and Christopher J. Carroll

Open File Report 2017-6
September 2017

Wyoming State Geological Survey

Thomas A. Drean, Director and State Geologist

Preliminary Geologic Map of the Bridger Pass Quadrangle, Carbon County, Wyoming

By Derek T. Lichtner, Jacob D. Carnes, Seth J. Wittke, and Christopher J. Carroll

Layout by Christina D. George

Open File Report 2017-6
Wyoming State Geological Survey
Laramie, Wyoming: 2017

This Wyoming State Geological Survey (WSGS) Open File Report is preliminary and may require additional compilation and analysis. Additional data and review may be provided in subsequent years. For more information about the WSGS, or to download a copy of this Open File Report, visit www.wsgs.wyo.gov. The WSGS welcomes any comments and suggestions on this research. Please contact the WSGS at 307-766-2286, or email wsgs-info@wyo.gov.

Citation: Lichtner, D.T., Carnes, J.D., Wittke, S.J., and Carroll, C.J., 2017, Preliminary geologic map of the Bridger Pass quadrangle, Carbon County, Wyoming: Wyoming State Geological Survey, Open File Report 2017-6, 41 p., scale 1:24,000.

Table of Contents

Introduction 1
Location. 1
Geologic Setting 2
Structure 3
Economics 4
Petroleum 4
Coal 5
Industrial Materials 7
Bentonite. 7
Zeolite. 7
Aggregate. 7
Uranium. 7
Description of Map Units 8
Cenozoic Deposits and Sedimentary Rocks 8
Mesozoic Sedimentary Rocks 10
References 21
Appendix 1: Preliminary Petrographic Analysis 25
Appendix 2: Coal Quality Analysis 33
Appendix 3: Source Rock Analysis. 40

List of Figures

Figure 1. Anticline in Haystack Mountains Formation 3
Figure 2. Normal fault that offsets sandstones in Haystack Mountains Formation. 4
Figure 3. Landslide terrain along northern escarpment of Miller Hill 8
Figure 4. Pediment gravels in foreground, west of Atlantic Rim. 9
Figure 5. Outcrop of Browns Park Formation basal conglomerate 9
Figure 6. Streamcut through Lewis Shale. 10
Figure 7. Coals in Almond Formation 11
Figure 8. Jep Canyon, where all formations within Mesaverde Group are exposed. 12
Figure 9. Outcrop of Pine Ridge sandstone 13
Figure 10. Allen Ridge Formation. 14
Figure 11. Haystack Mountains Formation sandstones 15

Figure 12. Streamcut through Steele Shale 16
Figure 13. Wolf Mountain bench of Niobrara Formation 17
Figure 14. Niobrara Formation outcrop west of Miller Hill 17
Figure 15. Outcrop of Mowry Shale in Stoney Creek drainage atop Miller Hill 18
Figure 16. Chert conglomerate and crossbedded sandstones at base of Cloverly Formation. 19
Figure 17. Lower Cretaceous and Jurassic formations in Grove Creek drainage atop Miller Hill 20

List of Tables

Table 1. WOGCC records for oil and gas wells completed within the Bridger Pass quadrangle 6

INTRODUCTION

The goal of this study was to further understanding of Cretaceous stratigraphy in the Atlantic Rim area, where future development of coal and coalbed resources is anticipated (BLM, 2007). This goal was accomplished through detailed mapping of the bedrock geology in the Bridger Pass 7.5' quadrangle, approximately 19 miles southwest of Rawlins, Wyoming. Comprehensive delineation of this region's stratigraphy and structure may facilitate not only current oil and gas production but also identify areas for potential development. New and updated geologic maps may also provide a base for further exploration of other mineral resources, including uranium.

Previous geologic mapping in the Bridger Pass area is limited in scope and detail. Collier (1925), Buehner (1936), and Larson and Vieaux (1951) led the first moderately detailed mapping efforts in the region; these data were compiled on a geologic map of Carbon County (Weitz and Love, 1953). Love (1953) conducted a preliminary assessment of uranium resources in the Miller Hill area. Vine and Prichard (1959) followed this preliminary assessment with a comprehensive report on uranium occurrences; their map contains the southeast corner of the Bridger Pass quadrangle. Berry (1960) investigated groundwater resources in the Rawlins area, including the eastern two-thirds of the quadrangle.

In the 1970s and 1980s, C.S.V. Barclay oversaw field work at the Bridger Pass quadrangle and several surrounding quadrangles; Barclay's data were unpublished until recently, when his field notes and sketches were compiled and released by the U.S. Geological Survey (USGS; Haacke and others, 2016). Hettinger and others (2008) compiled and mapped coalbed stratigraphy in the Atlantic Rim region, focusing on the Paleocene Fort Union Formation. McLaughlin and Fruhwirth (2008) compiled and mapped the geology of the Rawlins 1:100,000-scale quadrangle; however, their map does not present in detail the geology near Bridger Pass. Quillinan and others (2009) compiled a map of coal bed natural gas activity in the Atlantic Rim area; their map also does not depict the Bridger Pass area in detail.

Mapping for this study consisted of on-the-ground examination of rock units, interpretation of satellite imagery, and compilation of previously published and unpublished maps and reports. Field work was conducted between September 2016 and August 2017. Mapping was completed in cooperation with the USGS StateMap grant award G16AC00199.

We wish to acknowledge and thank Blake Sheep Co., Overland Trail Land & Cattle Co., and PH Livestock Co. for access to their private lands. This project would not have been possible without their generosity.

LOCATION

The geography of south-central Wyoming is defined by the intersection of several contrasting landscapes. To the northwest of the map area, the Great Divide Basin, a Laramide structure, is filled with nearly flat-lying Eocene and older rocks. The Washakie Basin, another Laramide basin, stretches for upward of 50 miles to the southwest. To the north, the predominantly Paleozoic rocks of the Rawlins Uplift overlook U.S. Interstate 80. To the southeast, the broad Precambrian peaks of the Sierra Madre Range—a northern extension of Colorado's Park Range—rise above the dissected plateau of Miller Hill, an erosional remnant of Miocene rock that itself towers a thousand feet above the surrounding sagebrush plains. Near the center of the map, Bridger Pass Road rolls over a subtle rise that separates Emigrant Creek from a tributary of McKinney Creek. From this inconspicuous divide, Emigrant Creek flows northeast to the North Platte River, whose waters eventually make their way to the Gulf of Mexico, while McKinney Creek flows southwest to the Little Snake River, and ultimately to the Gulf of California.

The Atlantic Rim is a prominent ridge that bisects the map area, exemplifying this meeting of landscapes. Composed of resistant Mesaverde Group sandstones, the Atlantic Rim rises up to 240 m (800 ft) above flanking valleys of Cretaceous shale. Although vegetation in the area is sparse, conifer and deciduous trees survive in sheltered valleys and on north-facing slopes of the rim. The ridge-forming Mesaverde dips gently to the west, where it is buried by

thousands of meters of basin fill. Thus, the Bridger Pass area embodies the boundary between Laramide uplift and basin.

The map area is in Carbon County, Wyoming, and encompasses the entirety of the Bridger Pass 7.5' quadrangle (Tps. 18–19 N. and Rgs. 89–90 W.). The general region is accessible via Wyoming Highway 71 (Sage Creek Road). Several roads provide access to the map area, including Bureau of Land Management (BLM) Road 3301 (Bridger Pass Road), County Road 505W (Miller Hill Road), and County Road 605N (Twenty Mile Road). The northeast corner of the quadrangle is approximately 20 km (13 mi) southwest of Rawlins, Wyoming.

The quadrangle is within the "checkerboard," an area where land ownership alternates, section by section, between privately held land and public land managed by the BLM and the State of Wyoming. Permission must be obtained from landowners prior to entering private lands.

GEOLOGIC SETTING

The Jurassic and Cretaceous strata exposed in the map area record the advance and retreat of epicontinental seaways during the Mesozoic. During Sundance time (Middle and Upper Jurassic), two major transgressions and regressions occurred over the stable Wyoming shelf (Picard, 1993). The Sundance seas were then followed by the alluvial fans, braided and meandering streams, and ephemeral lakes of the Morrison Formation, the uppermost Jurassic unit in the Bridger Pass quadrangle (Picard, 1993).

Cretaceous rocks at Bridger Pass record deposition in the Sevier foreland basin, which formed as a flexural response to crustal loading imposed by the Sevier orogenic belt to the west (Steidtmann, 1993). Bentonite, sourced from Sevier-related volcanic activity, is common throughout Cretaceous units. The beginning of the area's Cretaceous record is marked by the gravels of the Cloverly Formation, which originated from the fold-and-thrust belt and spread northeast across the foreland basin. Deposition of the Cloverly was followed by a short-lived transgression of the Western Interior Seaway, during which time the Thermopolis Shale was deposited. A brief regression followed, and incised valleys were filled with the thin deposits of the Muddy Sandstone. The Mowry Sea then flooded the foreland from the north; this seaway was stagnant and relatively deep, facilitating the deposition of dark organic-rich shale.

Eustatic sea level continued to rise, reaching its highest level at the beginning of the Late Cretaceous (Steidtmann, 1993). Progradation of shallow- and marginal-marine sediments into this extensive seaway resulted in the deposition of the sandstones and siltstones of the Frontier Formation. The Niobrara transgression followed, and the seaway reached its second-highest level of the Cretaceous, resulting in the widespread and thick deposits of the Niobrara Formation, Steele Shale, and laterally equivalent chalks, marls, and shales. Regression of the Niobrara seaway is marked by deposition of the Mesaverde Group and the progradation of fluvial, coastal, marginal-marine, and near-shore environments into the foreland basin. More frequent, smaller-scale transgressions and regressions within the Mesaverde Group do not appear to correspond directly to eustatic sea level and may reflect local tectonic influences (Roehler, 1990; Martinsen and others, 1993). Deposition of the Mesaverde Group was followed by the final advance and retreat of the Western Interior Seaway, during which the Lewis Shale was deposited. The ultimate transition from marine to non-marine environments is recorded by the deltaic deposits of the Fox Hills Sandstone, which is exposed less than a kilometer northwest of the map area. For the remainder of the Cretaceous, non-marine conditions prevailed.

Near the end of the Cretaceous, the Laramide orogeny began, partitioning Wyoming into structural basins separated by Precambrian-cored uplifts. During much of the Paleogene, the exhumation of these uplifts produced thick sections of basin fill, covering the Jurassic and Cretaceous strata in many locations. These latest Cretaceous through Oligocene strata are not preserved in the map area. Rather, Neogene uplift, erosion, and resultant shedding of alluvial sediment from the nearby Sierra Madre and Park Ranges resulted in the deposition of the Miocene(?) Browns Park Formation. This youngest consolidated unit in the map area rests on an uneven surface cut into the Cretaceous and Jurassic units atop Miller Hill. In the late Miocene, the region experienced extensional faulting

(Buffler, 1967; Montagne, 1991). In more recent times, the rocks at Bridger Pass have been eroded, reworked, and deposited as alluvium, colluvium, and pediment gravels.

STRUCTURE

Geologic structure in the Bridger Pass quadrangle is controlled by its location at the margins of the Great Divide and Washakie basins—together comprising the eastern portion of the Greater Green River Basin—and the Sierra Madre Range. The inclinations of strata in the map area range from 4°–26°, dipping northwest to west, away from the Sierra Madre and toward the basins. Wamsutter Arch—a west-east trending subsurface anticline that separates the Great Divide and Washakie basins—is due west of the map area. Broad synclinal and anticlinal basinward-plunging folds, their hinge axes perpendicular to the basin margin, modulate strata strikes and dips along the Atlantic Rim (Hettinger and others, 2008). One such anticline (fig. 1) occurs near the northeastern corner of the Bridger Pass quadrangle, beneath the Espy Unit exploratory oil field.

Figure 1. Anticline in Haystack Mountains Formation, T. 19 N., R. 89 W., sec. 23, looking northwest. Much of the oil production in the Bridger Pass quadrangle is from wells that penetrate this subtle structure.

Normal faults in the region also tend to be orientated perpendicular to the basin margin. One such fault (fig. 2) occurs in the southwest portion of the map area, centered in T. 18 N., R. 90 W., sec. 13, and offsets strata in the Mesaverde Group, from the Haystack Mountains Formation through the Almond Formation. The fault seems to disappear within the shale between the lowermost Seminoe Sandstone and the O'Brien Spring Sandstone of the Haystack Mountains Formation.

Other faults in the region, although rare, are parallel, rather than perpendicular, to the basin margin (Hettinger and others, 2008). One such fault occurs in T. 19 N., R. 90 W., sec. 24, near the contact between the Lewis Shale and underlying Almond Formation. Hettinger and others (2008) inferred this fault to be a normal fault, with the downthrown block in the direction of the basin (northwest). However, this study found the offset, depth, and overall

Figure 2. Normal fault that offsets sandstones in the Haystack Mountains Formation, T. 18 N., R. 89 W., sec. 18, looking west. The downthrown block is to the north (right).

attitude of the fault difficult to determine from either surface or subsurface data. Extensive study of fracture and jointing trends was not conducted as part of these mapping activities. However, those attitude measurements collected are generally subvertical and oriented perpendicular to the strike of bedding. Many of these fractures feature iron-stained surfaces.

The geologic structure in the Bridger Pass quadrangle increases in complexity away from the basin margin. The Miller Hill/Hatfield Dome Anticline plunges northward beneath Miller Hill, at the southeast corner of the map area. This anticline terminates at the complexly faulted southern end of the Rawlins Uplift, 10 miles north of the map boundary (Vine and Prichard, 1959). Only the western limb of this anticline is observed in the Bridger Pass quadrangle, in streamcuts through the Cretaceous and Jurassic strata beneath Miller Hill. East of the map area, geologic structure is dominated by the Sierra Madre and Medicine Bow uplifts, whereas north of the map area, structure is controlled by the Rawlins Uplift.

ECONOMICS

Petroleum

More than 5,000 oil and gas wells have been completed in the nearby Washakie Basin (WOGCC, 2017). Current targets include coalbed natural gas from Cretaceous Mesaverde Group coals near the basin margin (Quillinan and others, 2009) and more deeply sourced natural gas in the low-permeability ("tight gas") sandstones of the Mesaverde Group, Cretaceous Lance Formation, and Paleocene Fort Union Formation (McDonald, 1975; Bircher, 2014; Lynds and others, 2015; Lynds and Lichtner, 2016). Coalbed natural gas has been produced from Mesaverde Group coals less than 3.2 km (2 mi) west and 6.4 km (4 mi) north of the Bridger Pass quadrangle, from the Jolly Roger and Red

Rim units, respectively. These units are part of the 270,080-acre Atlantic Rim Natural Gas Field Development Project, a 50-mi long corridor of coalbed natural gas activity on the margin of the Washakie Basin. The BLM's Atlantic Rim development plan (BLM, 2007) anticipates that up to 2,000 wells will produce nearly 1,350 billion cubic feet (bcf) of natural gas. As of July 2017, the Wyoming Oil and Gas Conservation Commission (WOGCC) lists 449 completed coalbed natural gas wells in the development area (WOGCC, 2017). Seventy-two of these wells are plugged and abandoned, while 281 are listed as producing gas from Allen Ridge or Almond coal seams. Since the late 1990s, when the Atlantic Rim was first targeted for coalbed methane development, approximately 165 bcf of gas and 679 million barrels (MMbbls) of water have been produced from Mesaverde coals. Many of the currently producing wells are operated by Warren Resources, Inc. or Escalera Resources Co.

Oil and gas wells within the Bridger Pass quadrangle target deeper conventional reservoirs than the nearby coalbed natural gas activity. Since 1956, 28 exploration wells have been completed in the quadrangle (table 1). As of July 2017, 17 of these wells are permanently abandoned and three are temporarily shut-in or abandoned. One well status is indicated as "pumping rods." Seven wells are listed by the WOGCC as active and producing oil and/or gas from the Niobrara, Frontier, and Tensleep formations. These active wells are all within Espy Field and operated by Thorofare Resources, Inc.

Coal

Coal-bearing units in the Bridger Pass quadrangle include the Allen Ridge and Almond formations (Dames and Moore, 1978). Coals in the Allen Ridge Formation occur in the upper portion of the unit. Allen Ridge coals are associated with carbonaceous shale and range from 0.3–1.2 m (1–4 ft) in thickness.

Using drill-hole data, Dames and Moore (1978) identified four persistent coal beds within the Bridger Pass quadrangle, all in the Almond Formation. The thickest Almond Formation coals occur in the lower 200 ft of the formation, though coal is present in all parts of the unit.

The Z coal bed is the lowest persistent coal of the Almond Formation. The Z coal typically occurs as two beds, the upper Z1 and lower Z2. The Z1 and Z2 beds are separated by approximately 6.1 m (20 ft) of shale and sandstone. The Z1 bed has an average thickness of 2 m (6 ft) in the Bridger Pass quadrangle and thins to the northeast. The Z2 bed ranges from 0.6–2.4 m (2–8 ft), and generally thins to the northeast and southwest.

The Y coal is 15–18 m (50–60 ft) above the Z2 coal. Maximum thickness of the Y coal observed in the Bridger Pass quadrangle is 2.7 m (9 ft), though the thickness of the Y coal ranges up to 4.5 m (15 ft) to the west of the quadrangle. The Y coal thins to the northeast and eventually pinches out.

The X coal is 12–17 m (40–55 ft) above the top of the Y coal, separated by interbedded sandstone and shale. Within the area of the Bridger Pass quadrangle, the X coal has a maximum thickness of about 2 m (6 ft) and pinches out to the northeast.

The W coal is the uppermost persistent Almond Formation coal bed in the Bridger Pass quadrangle. The typical thickness of the W coal is approximately 1.3 m (4 ft), but it may locally thicken up to 2 m (6 ft). The W coal is separated from the X coal by 12 m (40 ft) of interbedded shale and sandstone.

Dames and Moore (1978) calculated coal reserve base tonnages for federal lands within the Bridger Pass quadrangle. They developed separate estimates for areas of high, moderate, and low development potential (The development potential of an area is determined by the mining ratio, or the ratio of cubic yards of overburden per ton of recoverable coal. High development potential refers to an area with a mining ratio of 0 to 10, moderate is applied to ratios from 10 to 15, and mining ratios above 15 signal low development potential). In total, the reserve base for strippable high development potential coal is 4.826 million tonnes (5.32 million tons) on federal lands in the Bridger Pass quadrangle. For moderate development potential coal, the reserve base is 1.887 million tonnes (2.08 million tons),

Table 1. WOGCC records for oil and gas wells completed within the Bridger Pass quadrangle. Well status codes are as follows: "PA" = permanently abandoned, "PG" = producing gas, "PO" = producing oil, "PR" = pumping rods, "SI" = shut-in, "SR" = subsequent report of abandonment, and "TA" = temporarily abandoned.

API Number	Well Name	Company	Latitude (WGS84)	Longitude (WGS84)	Elevation KB (ft-msl)	Status	Total Depth (ft)	Oil (bbls)	Gas (Mcf)	Water (bbls)
49-007-05182	MILLER-HILL 2-1	SABINE OIL & GAS CORPORATION	41.557	-107.381	7,575	PA	3,820	-	-	-
49-007-05193	STATE 1	MCCULLOCH OIL	41.568	-107.395	7,340	PA	4,218	-	-	-
49-007-05200	UNIT 4	GKM INC	41.583	-107.401	7,554	PA	5,820	-	-	-
49-007-05206	UNIT 2	ATLANTIC RICHFIELD COMPANY	41.586	-107.453	8,350	PA	3,445	-	-	-
49-007-05210	UNIT UPRR 6	AMAX OIL AND GAS INC	41.593	-107.407	8,153	TA	5,980	-	-	-
49-007-05213	UNIT 1	ATLANTIC RICHFIELD COMPANY	41.594	-107.462	7,829	PA	10,515	-	-	-
49-007-05215	UNIT 3	THOROFARE RESOURCES INC	41.597	-107.394	-	SI	5,630	-	45,008	4,232
49-007-05217	UNIT 1	ATLANTIC RICHFIELD COMPANY	41.598	-107.391	7,628	PA	6,132	-	-	-
49-007-05221	ESPY UNIT 2	THOROFARE RESOURCES INC	41.601	-107.398	8,257	PR	4,023	18,089	27,375	2,290
49-007-05225	ESPY UNIT 1	THOROFARE RESOURCES INC	41.604	-107.398	8,291	PO	4,472	93,144	2,995	47,500
49-007-05227	ESPY UNIT 7	PEDCO RESOURCES COMPANY	41.608	-107.407	8,073	PA	6,001	-	-	-
49-007-05229	ESPY UNIT UPRR 5	THOROFARE RESOURCES INC	41.611	-107.393	8,432	PO	5,922	99,059	8,749	8,222
49-007-05235	ESPY UNIT 1	PRAY MAX	41.622	-107.408	8,095	PA	7,543	-	-	-
49-007-07121	ESPY UNIT 8	NADEL & GUSSMAN ROCKIES LLC	41.604	-107.383	7,710	SR	4,363	1,314	1,013	-
49-007-20102	UPRR-BOLTON RANCH 1	TENNECO OIL COMPANY	41.536	-107.443	7,389	PA	4,055	-	-	-
49-007-20116	UNIT 5	TENNECO OIL COMPANY	41.580	-107.487	7,689	PA	10,795	-	-	-
49-007-20149	FEDERAL 34-1	READY ROGER	41.583	-107.396	7,453	PA	3,800	-	-	-
49-007-20151	CHAMPLIN-MCKAY 27-1	OGLE CORPORATION	41.590	-107.396	7,542	PA	4,511	-	-	-
49-007-20237	ESPY UNIT 9	THOROFARE RESOURCES INC	41.604	-107.394	8,360	PO	8,629	184,834	35,445	2,006,019
49-007-20339	ESPY UNIT 10	AMAX OIL AND GAS INC	41.608	-107.398	8,376	PA	4,095	-	-	-
49-007-21470	ESPY 14-23	THOROFARE RESOURCES INC	41.602	-107.387	7,933	SI	4,900	54,158	8,161	7,334
49-007-21534	ESPY 10-15	THOROFARE RESOURCES INC	41.619	-107.403	8,220	PA	5,905	-	-	-
49-007-21535	ESPY 1-22	THOROFARE RESOURCES INC	41.611	-107.399	8,333	PO	8,509	52,262	-	220
49-007-22770	SUGAR CREEK 1	SCHOLL ROBERT G	41.598	-107.473	7,467	SR	9,000	-	-	-
49-007-23719	ESPY 12	THOROFARE RESOURCES INC	41.598	-107.388	7,563	PO	8,035	143,715	-	2,006,581
49-007-23721	ESPY 13	THOROFARE RESOURCES INC	41.617	-107.393	8,432	PO	8,753	78,455	-	442,431
49-007-24032	ESPY 15	THOROFARE RESOURCES INC	41.608	-107.392	-	PG	6,377	-	65,195	-
49-007-60028	ESPY UNIT 10	LADD & LUKOWICZ	41.608	-107.398	8,330	PA	4,095	-	-	-

and for low development potential, 6.722 million tonnes (7.41 million tons). The total reserve base is highest for the Y coal bed at 5.606 million tonnes (66.18 million tons), followed by the Z1 coal at 4.872 million tonnes (5.37 million tons). The Z2 coal has a reserve base of 1.742 million tonnes (1.92 million tons). Where the Z coal is not split, its reserve base is 644,000 tonnes (710,000), and the reserve base for the X coal is 562,000 tonnes (620,000 tons).

Due to poor exposure, coal beds in the Bridger Pass quadrangle are difficult to distinguish in the field; Wyoming State Geological Survey (WSGS) geologists made no effort to identify outcrops of these four named coal beds.

Industrial Materials

The area does not have known deposits of abundant industrial minerals; however, potential bentonite, zeolite, and aggregate sources are summarized below.

Bentonite

Previous work describes bentonitic zones and layers within several map area units, including the Lewis, Steele, and Mowry shales, and the Cloverly Formation (Love, 1953; Vine and Prichard, 1959; Gill and others, 1970; Carroll and others, 2015). The Steele Shale contains beds of bentonite up to 1.5 m (5 ft) thick (Gill and others, 1970). Although WSGS geologists noted bentonitic material in the Steele Shale at Bridger Pass, no clear bentonite beds were observed due to poor exposure.

The Mowry Shale is capped by the Clay Spur Bentonite, a thick and extensive bentonite deposit of economic interest. In the Bridger Pass quadrangle, the Clay Spur Bentonite is covered by the Miocene Browns Park Formation. An active bentonite mine in the Mowry Shale is located approximately 13 mi southwest of the map area in T. 16 N., R. 87, W. (Harris, 2004).

Zeolite

The Browns Park Formation contains zeolitic tuffs in the Saratoga, Pick Ranch, Pick Bridge, and Poison Basin areas (King and Harris, 2002; Gregory and others, 2016). Exposure of the Browns Park at Bridger Pass is limited mostly to its basal conglomerate, which is of alluvial origin. No tuff samples suitable for zeolite analysis were observed in the study area. Harris (2004) indicates zeolite deposits in the Miocene rocks of the region may be found in outcrops several miles southeast of the map area, where the upper sequence of the Browns Park Formation is preserved.

Aggregate

Alluvial gravels and other such deposits are scarce in the Bridger Pass area. Harris (2004) documented a pit quarry for sand, gravel, or unspecified aggregate near T. 18 N., R. 87 W., sec. 10, about 9 mi east of the map area.

Uranium

Love (1953) and Vine and Prichard (1959) describe uranium deposits in the Miocene Browns Park Formation on Miller Hill. The known uranium occurrences on Miller Hill are outside the map area. The highest uranium concentrations occur within brecciated, silicified limestone beds that range from 0.9–3.0 m (3–10 ft) in thickness. Lower uranium concentrations occur in limonite-stained calcareous sandstone and orthoquartzite. In the brecciated, silicified limestone, the uranium mineral uranophane [$Ca(UO_2)_2(HSiO_4)_2 \cdot 5H_2O$] coats fractures and vugs. In the sandstones, the uranophane is disseminated. Uranium is also detectable in lenses and irregular masses of chert and chalcedony. Maximum uranium concentrations in the brecciated, silicified limestone beds of the Browns Park Formation are about 0.1 percent uranium. Maximum uranium concentrations in other lithologies are 0.01–0.02 percent uranium. Two beds of brecciated, silicified limestone account for most of the radioactivity anomalies on Miller Hill. These two beds occur approximately 84 m (275 ft) and 125 m (410 ft) above the basal conglomerate of the Browns Park Formation. The stratigraphic intervals of the two limestone beds are likely not preserved within

the map area; during field investigations, WSGS geologists did not observe brecciated, silicified limestone, or radioactive anomalies.

DESCRIPTION OF MAP UNITS

Cenozoic Deposits and Sedimentary Rocks

Quaternary

Alluvium (Qal)

The material mapped as alluvium in the Bridger Pass quadrangle consists of unconsolidated sand, silt, clay, and coarse gravels and cobbles, mainly along floodplains and ephemeral streams. Alluvium is mapped beside Grove Creek and Stoney Creek atop Miller Hill, Eagle Creek immediately west of Miller Hill, McKinney Creek near Bridger Pass Road, and Separation Creek, in both Jep Canyon and alongside County Road 605N (Twenty Mile Road). All mapped alluvial material is derived locally and generally ranges up to 8 m (26 ft) thick.

Alluvium and Colluvium, undivided (Qac)

Undivided alluvium and colluvium is mapped at the bases of slopes and along steep-sided, intermittent headwater drainages. This unit consists of unconsolidated clay, silt, sand, and gravel. The alluvium and colluvium are derived locally and are often capped by soil and relatively dense vegetation. Thickness is generally less than 8 m (26 ft).

Landslide material (Qls)

Quaternary landslides are confined primarily to the north- and west-facing escarpments of Miller Hill (fig. 3), where the basal conglomerate of the Browns Park Formation overlies Upper Cretaceous shales, and to escarpments along the Atlantic Rim, where sandstones of the Haystack Mountains and Almond formations overlie shales within these same formations. The shales in both locations become saturated and slump down the steep slopes situated beneath the resistant sandstones and conglomerates. The landslide debris is typically a mixture of Cretaceous shales and sandstones and Miocene(?) sandstone and conglomerate.

Figure 3. Landslide terrain along the northern escarpment of Miller Hill, T. 18 N., R. 89 W., sec. 15.

Pediment deposits (QTp)

Pediment deposits are smooth surfaces, dipping gently west, that are located between the western flank of the Atlantic Rim and Separation Creek. Pediment material consists of unconsolidated subangular clasts, derived from local Almond Formation and Lewis Shale sandstone bodies, in a sandy matrix (fig. 4). These deposits are less than 3 m (10 ft) thick.

Figure 4. Pediment gravels in foreground, west of the Atlantic Rim, T. 19 N., R. 90 W., sec. 24. Lewis Shale and Fox Hills Sandstone crop out in the distance, outside the map area.

Miocene

Browns Park Formation (Tbp)

The Browns Park Formation is composed of two parts: a basal conglomerate and an overlying sequence of assorted sandstones, mudstones, and algal limestones. The upper part is composed chiefly of gray-yellow, horizontally stratified, flaggy, very fine to medium-grained sandstone. These sandstones vary in hardness and resistance to weathering, and may be locally calcareous or silicified. Vine and Prichard (1959) describe an assortment of other components, including siltstones, eolian sandstones, and algal limestones; these lithologies were not observed in the Bridger Pass quadrangle, and are either poorly exposed or limited to the uppermost portions of the formation, which are not present in the map area. Outcrops of the upper part of the Browns Park Formation in the Bridger Pass quadrangle consist of a few isolated mounds atop Miller Hill. Exposure is generally very poor and limited mostly to areas of concentrated float.

Figure 5. Outcrop of Browns Park Formation basal conglomerate, T. 18 N., R. 90 W., sec. 13.

The conglomerate consists predominantly of subrounded white quartzite clasts, with varying amounts of limestone, granitoids, gneiss, and chert in a friable, poorly sorted silt and sand matrix (fig. 5). The white quartzite clasts are perhaps the most pervasive component of the basal conglomerate. Granitoid boulders may be up to 1 m (3 ft) in diameter. Pebble conglomerates and coarse sandstones alternate and interfinger within the basal conglomerate. Graded bedding is common. The basal conglomerate caps Miller Hill

as well as a small butte in the southwest corner of the quadrangle. Despite the conglomerate's apparent resistance to weathering, the quality of outcrop is generally poor.

The Browns Park Formation was deposited 23.5–14.5 Ma (Montagne, 1991); however, correlation from exposures in the Bridger Pass quadrangle to age-constrained outcrops in the Saratoga Valley remains difficult. Some debate also appears to exist as to whether the Miocene(?) rocks in the map area are actually Browns Park Formation. While Vine and Prichard (1959) map the rocks atop Miller Hill as the "North Park Formation(?)," the authors of this report follow Montagne's (1991) conclusion that "Browns Park Formation," as described on Love and Christiansen's (1985) geologic map of Wyoming, remains the most useful designation for Miocene(?)-age, primarily alluvially derived rocks in and around the Saratoga Valley.

The deposits of the Browns Park Formation reflect a variety of environments. The basal conglomerate was deposited by debris and alluvial flows. Its clasts are predominantly Precambrian in origin and were derived from the Park and Sierra Madre ranges; the quartzite clasts in particular suggest an origin from the white quartz veins that cut the igneous and metamorphic rocks to the southeast (Vine and Prichard, 1959; Montagne, 1991). The upper portion of the formation reflects localized alluvial, lacustrine, and eolian deposition (Vine and Prichard, 1959; Montagne, 1991). Prevailing westerly winds in mid- to late-Neogene carried deposited ash from volcanically active regions to the west, and thus volcanic ash is present throughout the formation (Luft and Thoen, 1981; Luft, 1985).

The basal conglomerate is up to 90 m (300 ft) thick. Because of the uneven, unconformable surface on which the Browns Park was deposited, the thickness of the upper part of the formation in the Bridger Pass quadrangle remains undetermined. Based on outcrops south of the Bridger Pass area, where the upper part of the formation is better exposed, Vine and Prichard (1959) report a total thickness of at least 240 m (790 ft).

Mesozoic Sedimentary Rocks

Upper Cretaceous

Lewis Shale (Kle)

The Lewis Shale is a gray to dark-gray shale, weathering light yellow-gray, interbedded with occasional thin, yellow-gray sandstones (fig. 6). Exposure is poor; the Lewis forms the flat, broad valley occupied by Separation Creek and its tributaries. The Dad Sandstone Member (Perman, 1987; Pyles and Slatt, 2000; Carroll and others, 2016) was not observed in the map area.

Figure 6. Streamcut through Lewis Shale, T. 19 N., R. 89 W., sec. 13.

The Lewis Shale was deposited 71–69 Ma during the final transgression of the Western Interior Seaway northwest into the Hallville embayment (Perman, 1987; Roehler, 1990). In the Bridger Pass quadrangle, it is approximately 700 m (2,300 ft) thick. The contact between the Lewis Shale and the underlying Almond Formation is sharp and conform-

able, and most easily recognized by the break in slope between the flat valley of Lewis Shale and the ridge-forming Mesaverde Group.

Mesaverde Group (Kal, Kpr, Kar, Khm)

Almond Formation (Kal): The Almond Formation is composed of brown-gray, very fine grained sandstone interbedded with gray-brown mudstone, carbonaceous shale, and coal. The sandstones are cross- and subplanar-bedded and contain occasional lithic clasts, up to 1 cm (0.4 in) in diameter, of mudstone and shale. Trace fossils are common, particularly *Planolites* and *Ophiomorpha*, and increase in frequency upsection. Occasional bivalve fossils are present throughout. Rare honeycomb weathering was observed. Soft sediment deformation, particularly water escape structures, are present in the lower sandstones. Sandstone and mudstone intervals are several meters thick near the base of the formation; the sandstones become thinner and less frequent upsection. Discontinuous coal beds, ranging in thickness from centimeters up to 1.5 m (5 ft), are common within carbonaceous zones (fig. 7). Outcrops weather in a striped pattern. Near Bridger Pass, Almond Formation sandstones form the ridgeline northwest of Jep Canyon (fig. 8).

Figure 7. Coals in the Almond Formation, T. 19 N., R. 89. W., sec. 9.

Figure 8. Jep Canyon, where all formations within the Mesaverde Group are exposed, T. 18 N., R 90 W., sec. 12.

The Almond Formation was deposited 72.4– 70.4 Ma during a period of overall transgression (Luo and Nummedal, 2010). At its base, the Almond is composed of coastal plain deposits. Upsection, the environment of deposition transitions to an estuarine barrier plain and ultimately to a marine shoreline. In the Bridger Pass quadrangle, the Almond Formation is approximately 300 m (980 ft) thick. The Almond is equivalent to the upper part of the Williams Fork Formation in the Sand Wash Basin to the south (Rudolph and others, 2015).

The contact of the Almond Formation with the underlying Pine Ridge Sandstone is poorly exposed within the map area. Recent work in the region describes this contact as conformable and gradational (Carroll and others, 2015).

Pine Ridge Sandstone (Kpr): The Pine Ridge Sandstone is an overall fining-upward body of massive white-gray sandstone, medium- to very fine grained, with common trough cross-bedding (fig. 9). Cross sets are up to 0.6 m (2 ft) thick and decrease in thickness upsection. Occasional channel scours and clay-pebble lag deposits are present near the formation's base. Individual beds fine upward. Fossils are very rare. Honeycomb weathering is common. The quality of exposure in the map area is inconsistent. Where not covered by landslides or colluvium, the Pine Ridge Sandstone is exposed on the northwestern wall of Jep Canyon.

Figure 9. Outcrop of Pine Ridge sandstone, T. 18 N., R. 90 W., sec. 11.

The Pine Ridge Sandstone occupies a time span of 76.9–73.3 Ma and represents the fluvial and alluvial infilling of an incised valley (Martinsen, 1994; Luo and Nummedal, 2010). The Pine Ridge Sandstone is equivalent to the Canyon Creek Member of the Ericson Sandstone to the west, on the Rock Springs Uplift; the Teapot Sandstone Member of the Mesaverde Formation to the northeast, in the Powder River Basin; and the lower part of the Williams Fork Formation to the south, in the Sand Wash Basin (Rudolph and others, 2015). The formation's thickness is variable (Roehler, 1990; Carroll and others, 2015). Within the map area, the Pine Ridge Sandstone is no thicker than 45 m (150 ft).

The contact of the Pine Ridge Sandstone with the underlying Allen Ridge Formation is sharp and unconformable. Approximately 3.5 million years of erosion and/or non-deposition—caused by localized, incipient Laramide movements—separate the Pine Ridge from the Allen Ridge (Luo and Nummedal, 2010; Rudolph and others, 2015).

Allen Ridge Formation (Kar): The Allen Ridge Formation is composed of brown-orange shale, mudstone, and siltstone interbedded with very fine grained gray sandstone lenses that weather rust orange. The sandstones contain

occasional wavy bedding and ripple laminations. Iron-oxide concretions are common and may be as large as 5 cm (2 in) in diameter. The lower portion of the Allen Ridge is poorly exposed, forming gentle slopes of shale covered in thin sandstone and siltstone rubble. The prominence of Allen Ridge sandstones increases upsection. The Allen Ridge Formation crops out in a striped pattern (fig. 10), which may be distinguished from the Almond Formation not only by the intervening Pine Ridge Sandstone—where well exposed—but also by the deep orange-brown of Allen Ridge siltstones and mudstones compared to gray-brown Almond shales. Within the map area, the lower portion of the Allen Ridge underlies the floor and east flank of Jep Canyon, while the upper portion is exposed in the ridge northwest of Jep Canyon.

Figure 10. Allen Ridge Formation, T. 19 N., R. 89 W., sec. 15. The ridge in the background is composed of the Almond Formation.

The Allen Ridge Formation was deposited 77.4–73.3 Ma in flood and coastal plain environments during an overall regression (Luo and Nummedal, 2010). Near Bridger Pass, the Allen Ridge Formation is approximately 290 m (950 ft) thick. To the south, in Colorado, the Allen Ridge is named the Iles Formation. To the east, it is equivalent to the lower part of the Rock River Formation, and to the west, it grades into the Trail Member of the Ericson Sandstone (Rudolph and others, 2015).

In some areas, the contact of the Allen Ridge Formation with the underlying Haystack Mountains Formation is considered an unconformity (Gomez-Veroiza and Steele, 2010; Rudolph and others, 2015); however, no clear unconformity was observed near Bridger Pass, where the contact is sharp and conformable. In this study, the basal contact was mapped between the uppermost white, coarsening-upward, nearshore sand body of the Haystack Mountains Formation, sometimes referred to as the unnamed sandstone member (Roehler, 1990), and the lowermost orange, coastal-plain channel sandstone of the Allen Ridge Formation.

Haystack Mountains Formation (Khm): The Haystack Mountains Formation is composed of gray-brown shale interbedded with very fine to fine-grained, coarsening-upward white-gray sandstones (fig. 11). Within the formation, there are up to 10 laterally pervasive sandstone tongues, often grouped into six zones: Tapers Ranch, Bolten Ranch, O'Brien Spring, Seminoe 1 though 4, Hatfield 1 and 2, and an unnamed uppermost member (Roehler, 1990; Mellere and Steel, 1995). These sandstone members were correlated from measured sections 2.4–9.6 km (1.5–6.0 mi) east-northeast of the Bridger Pass quadrangle (Gill and others, 1970; Mellere and Steel, 1995). This study mapped five sandstone zones; individual sandstone tongues were not differentiated. The Tapers Ranch Sandstone is composed of gray, hard, very fine grained, thinly bedded calcareous sandstone with occasional black lithic grains, rare glauconite, and thin bands of iron-oxide staining. The Bolten Ranch Sandstone was not observed; Mellere and Steel (1995) also do not observe this sandstone tongue in the area. The O'Brien Spring Sandstone is a friable, fine-grained sandstone rich in lithic fragments, giving unweathered surfaces a distinct salt-and-pepper appearance. The Seminoe Sandstones are a compact interval of interbedded sandstone and shale. Seminoe 1 consists of interbedded very fine grained trough-crossbedded white-gray sandstone that weathers gray-brown, gray-brown shale and thin

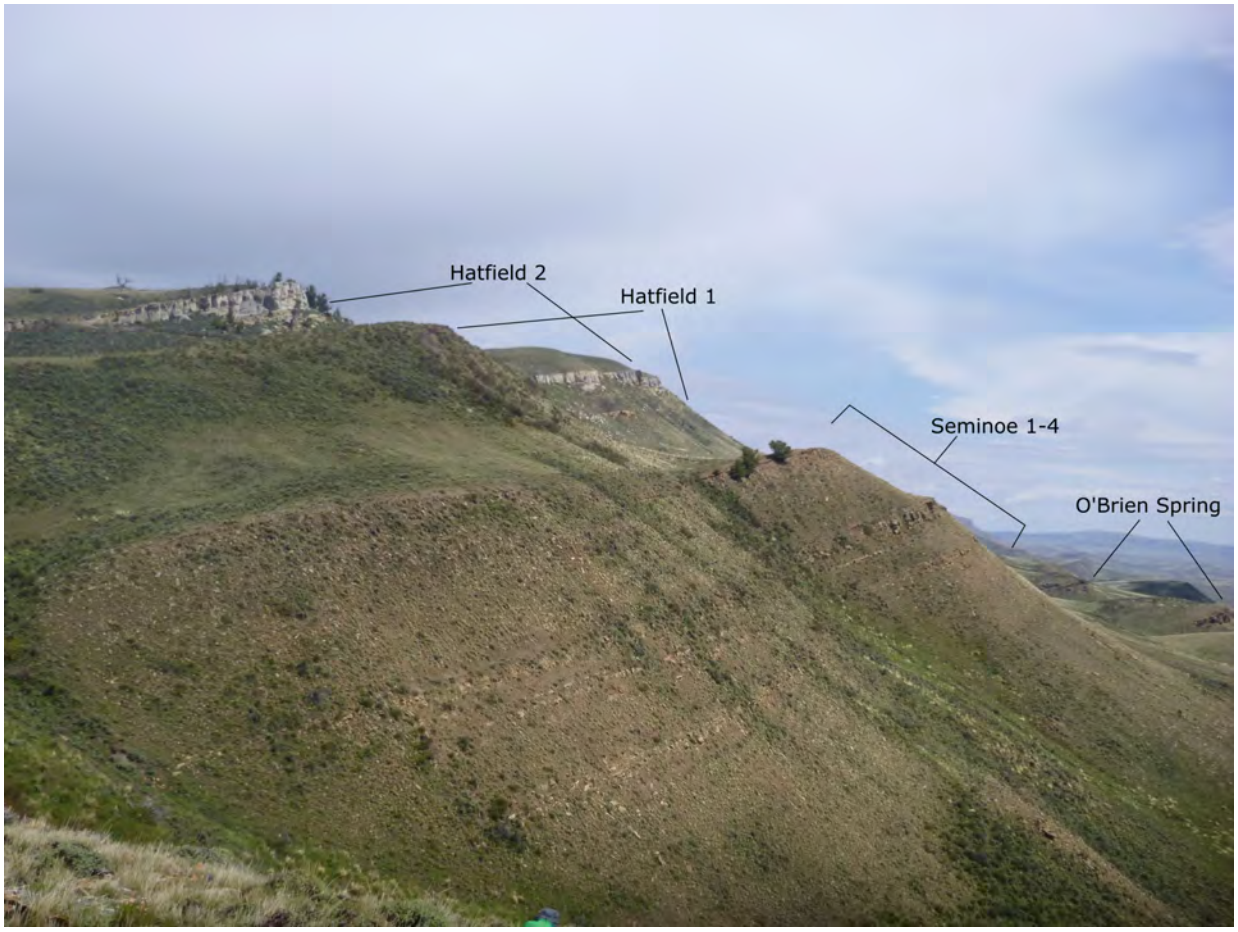

Figure 11. Haystack Mountains Formation sandstones, T. 18 N., R. 89 W., sec. 18.

sandstone, and fine- to medium-grained white gray sandstone with hummocky cross stratification. Seminoe 2 is a thin, rubbly, fine-grained sandstone similar to sandstones within the lower parts of Seminoe 1, but with more numerous lithic fragments. Seminoe 3 and 4 are similar to Seminoe 2, but more finely laminated and with fewer occurrences of lithic fragments. The Hatfield sandstones are both thick, cliff-forming sandstones separated by a thin shale. Hatfield 1 is a very fine grained gray sandstone that weathers gray-brown. It is thinly bedded at its base and becomes more flaggy and hummocky upsection. The top of the bed is bioturbated. Hatfield 2 is a thick, distinctly bleach-white, very fine to fine-grained, cross-bedded sandstone. The top of the bed is marked by 0.5 m (1.6 ft) of weathered red, medium-grained sandstone rich in disarticulated bivalve fossils, mostly oysters. Upsection of Hatfield 2, the Haystack Mountains Formation contains occasional signs of subaerial exposure, including mud cracks and at least one very thin coal, above which the uppermost prominent sandstone tongue—an unnamed sandstone that is massive, very fine to fine-grained, and bleach-white in color—was deposited. The top of this sandstone is also heavily bioturbated.

The sandstones within the Haystack Mountains Formation create a distinct series of stepped ridges comprising the east-facing escarpment of the Atlantic Rim, which, in most of the map area, is capped by prominent outcrops of Hatfield 2 Sandstone. The upper portion of the formation, above Hatfield 2, forms a gentle slope, subparallel to bedding, along the southeast side of Jep Canyon. Within the map area, the Haystack Mountains Formation is approximately 380 m (1,200 ft) thick.

The Haystack Mountains Formation was deposited 80.6–78.5 Ma during an overall regression (Luo and Nummedal, 2010). The sandstone tongues represent progradational, basinward-stepping nearshore and shoreface sand deposits embedded in marine shale. Near its top, the Haystack Mountains Formation is a mixture of coastal and near-

shore deposits. To the east, the Haystack Mountains Formation interbeds with and grades into the Steele Shale. To the west, in the Washakie Basin and on the Rock Springs Uplift, the formation grades into the nearshore and coastal deposits of the Blair and Rock Springs formations. Within the map area, the contact between the Haystack Mountains Formation and the underlying Steele Shale is gradational, and is mapped at the base of the lowermost laterally continuous nearshore sandstone, the Tapers Ranch Sandstone (Roehler, 1990).

Steele Shale (Ks): The Steele Shale is a dark-gray marine shale containing occasional lenticular beds of gray-brown sandstone that weather yellow-brown. Exposure is poor (fig. 12). The Steele forms the broad valley between the Atlantic Rim and Miller Hill. The upper part of the formation contains several thin sandstones that create small, rubbly ridges parallel to Bridger Pass Road.

Figure 12. Streamcut through Steele Shale, T. 19 N., R. 89 W., sec. 25.

The Steele Shale was deposited 85.1–80.6 Ma during transgression of the Western Interior Seaway (Luo and Nummedal, 2010). To the west, on the Rock Springs Uplift and in the Green River Basin, the Steele Shale is equivalent to the Baxter and Hilliard shales, respectively. To the south, in Colorado, it is equivalent to the Mancos Shale. To the north, throughout much of Wyoming and into Montana, the Steele Shale is equivalent to the upper parts of the Cody Shale. To the east, it is equivalent to the lower parts of the Pierre Shale. At Bridger Pass, the Steele Shale is approximately 820 m (2,700 ft) thick. The contact between the Steele Shale and the underlying Niobrara Formation is gradational and has been described as indistinct (Berry, 1960). Within the map area, the contact is mapped above the uppermost interval of hard, calcareous shale in the Niobrara Formation.

Niobrara Formation (Kn): The Niobrara Formation is a soft, dark-gray shale interbedded with white-gray calcareous shale and marl containing zones of calcite mineralization. These calcareous shales occur in three discrete zones; in northwestern Colorado, Vincelette and Foster (1992) informally refer to these zones, from oldest to youngest, as the Wolf Mountain, Tow Creek, and Buck Peak benches. These benches crop out as resistant ledges of hard, brittle shale (fig. 13), while the remainder of the Niobrara Formation forms the valley occupied by Eagle Creek (fig. 14). The complete thickness of the Niobrara Formation was not observed in the Bridger Pass quadrangle; the forma-

Figure 13. The Wolf Mountain bench of the Niobrara Formation, west of Miller Hill, T. 18 N., R.89 W., sec. 28.

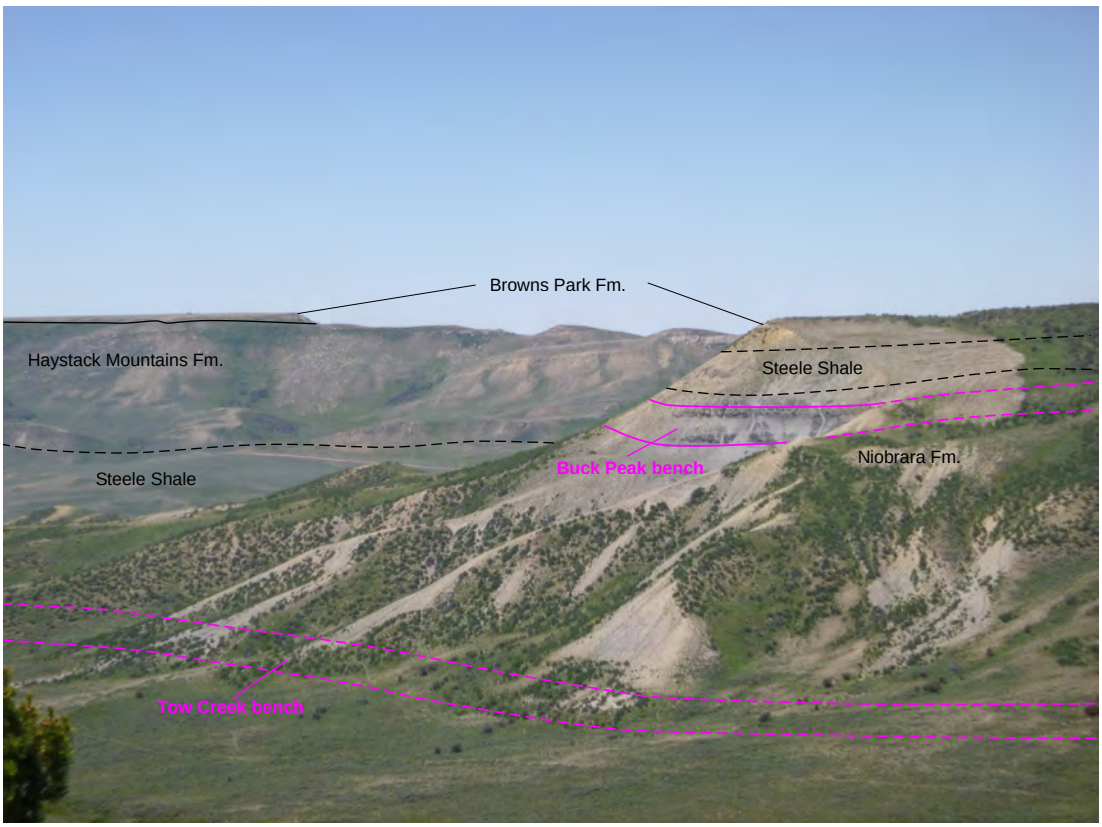

Figure 14. Niobrara Formation outcrop west of Miller Hill, T. 18 N., R.89 W., sec. 21.

tion's lowermost parts are covered by the Miocene Browns Park Formation. Subsurface data indicate a thickness of approximately 460 m (1,500 ft) for the combined Niobrara-Sage Breaks interval.

The age of the Niobrara Formation is 88.5–85.1 Ma (Luo and Nummedal, 2010). It was deposited during a major marine transgression when conditions were favorable for carbonate deposition. To the east, in the Denver-Julesburg Basin, chalks and limestones are the dominant lithologies (Finn and Johnson, 2005). In the Bridger Pass area, the composition of the Niobrara reflects a westward decrease in carbonate content and an increase in siliciclastic sediments derived from the Sevier orogenic belt to the west, near the modern-day Wyoming-Idaho state border (Vincelette and Foster, 1992). To the west and north, the Niobrara Formation grades into the noncalcareous shale and sandstone of the Baxter Shale (Finn and Johnson, 2005). The western limit of the calcareous facies of the Niobrara is not well known; it is thought to occur in the deeper parts of the Washakie and Great Divide basins (Finn and Johnson, 2005). The contact between the Niobrara Formation and the underlying Sage Breaks Shale was not observed in the Bridger Pass quadrangle; here, both the Sage Breaks Shale and most of the Frontier Formation are covered by Miocene Browns Park Formation. The contact between the Sage Breaks Shale and underlying Frontier Formation is gradational and generally placed at the top of the uppermost progradational sandstone (Kirschbaum and Roberts, 2005).

*Frontier Formation (*Kf): The Frontier Formation consists of interbedded gray-brown sandstone, gray shale, and thin lenticular beds of chert-pebble conglomerate. Exposure is limited to a single streamcut near the southern map boundary; elsewhere, the formation is covered by the Miocene Browns Park Formation. Because of this limited exposure, the Wall Creek, Emigrant Gap, and Belle Fourche members were not differentiated (Kirschbaum and Roberts, 2005), and the complete thickness was not observed. Vine and Prichard (1959) estimated a thickness of 210 m (700 ft) in the Miller Hill area, while subsurface data suggest a thickness closer to 170 m (560 ft).

The Frontier Formation was deposited 97–88.5 Ma during progradation of marginal-marine and marine sandstones into the Western Interior Seaway (Kirschbaum and Roberts, 2005). The contact between the Frontier Formation and the underlying Mowry Shale is sharp and conformable, and marked by the Clay Spur Bentonite, which is covered by Miocene Browns Park Formation in the Bridger Pass quadrangle (Kirschbaum and Roberts, 2005).

Mowry Shale (Kmr)

The Mowry Shale is a dark blue-gray, fissile, siliceous shale that weathers into distinct silver-colored plates, forming bare hillslopes paved with broken chips of shale (fig. 15). It is exposed in the southwestern corner of the map, where streamcuts along Stoney and Grove creeks reveal the Cretaceous and Jurassic strata beneath Miller Hill. Fossil fish scales are common (Vine and Prichard, 1959), although none were observed in the Bridger Pass quadrangle. The complete thickness of the Mowry Shale was not observed; the formation's uppermost parts are covered by the Miocene Browns Park Formation. Vine and Prichard (1959) estimated a thickness of 105 m (340 ft) for the Mowry near Miller Hill.

Figure 15. Outcrop of Mowry Shale in the Stoney Creek drainage atop Miller Hill, T. 18 N., R. 89 W., sec. 26.

The Mowry Shale was deposited 98.6–97 Ma during transgression of the Western Interior Seaway from the Artic Sea southward (Kirschbaum and Roberts, 2005). Radiolarians favored the cool waters of this Mowry sea; their silica tests were deposited on an anoxic sea floor, resulting in a siliceous shale (Davis, 1970). The shale grades upward and westward into bioturbated sandstone and mudstone (Kirschbaum and Roberts, 2005). The contact between the Mowry Shale and the underlying Thermopolis Shale is gradational and overall indistinct.

Lower Cretaceous

*Thermopolis Shale and Muddy Sandstone, undivided (*Kt): The Thermopolis Shale is a dark-gray soft shale interbedded in its upper half with the thin beds of gray, ferruginous Muddy Sandstone. Exposures are located in the far southwestern corner of the Bridger Pass quadrangle; these exposures are generally poor. Overall, the Thermopolis Shale forms gentle, vegetated slopes composed of soft, dark soil. The thin ferruginous sandstones of the Muddy Sandstone, which in previous mapping in the area have been grouped with the Thermopolis Shale, were not observed (Vine and Prichard, 1959).

The Thermopolis Shale and Muddy Sandstone were deposited from 99.5–98.6 Ma during a brief transgression and regression of the Western Interior Seaway (Kirschbaum and Roberts, 2005). The contact between the Thermopolis Shale and the underlying Cloverly Formation is conformable and is mapped above the "rusty beds" at the top of the Cloverly.

Cloverly Formation (Kcv): The Cloverly Formation consists of "rusty beds" of sandstone at its top, overlying bentonitic shale and a basal conglomerate. The sandstone is fine- to coarse-grained and white-gray with iron-oxide stains, weathering rusty brown. Individual beds within the sandstone are flaggy, subhorizontal, and approximately 5–15 cm (2–6 in) thick. The middle portion of shale is poorly exposed, forming a grassy, gently rolling surface littered with sandstone float. The lowermost part of the Cloverly Formation is a chert conglomerate, with smoky-gray quartzite and limestone clasts, interbedded with lenses of very fine to coarse-grained, crossbedded sandstone (fig. 16). The conglomerate and rusty sandstone are well exposed alongside Grove Creek, in the far southwestern corner of the Bridger Pass quadrangle (fig. 17). The Cloverly Formation in the map area is approximately 50 m (160 ft) thick.

The Cloverly Formation is Aptian to Albian in age and consists primarily of alluvial gravels sourced from the Sevier orogenic belt to the west (Steidtmann, 1993). The Cloverly grades into the Dakota Sandstone on the Rock Springs Uplift to the west (Kirschbaum and Roberts, 2005). The contact between the Cloverly Formation and the underlying Morrison Formation is sharp and unconformable.

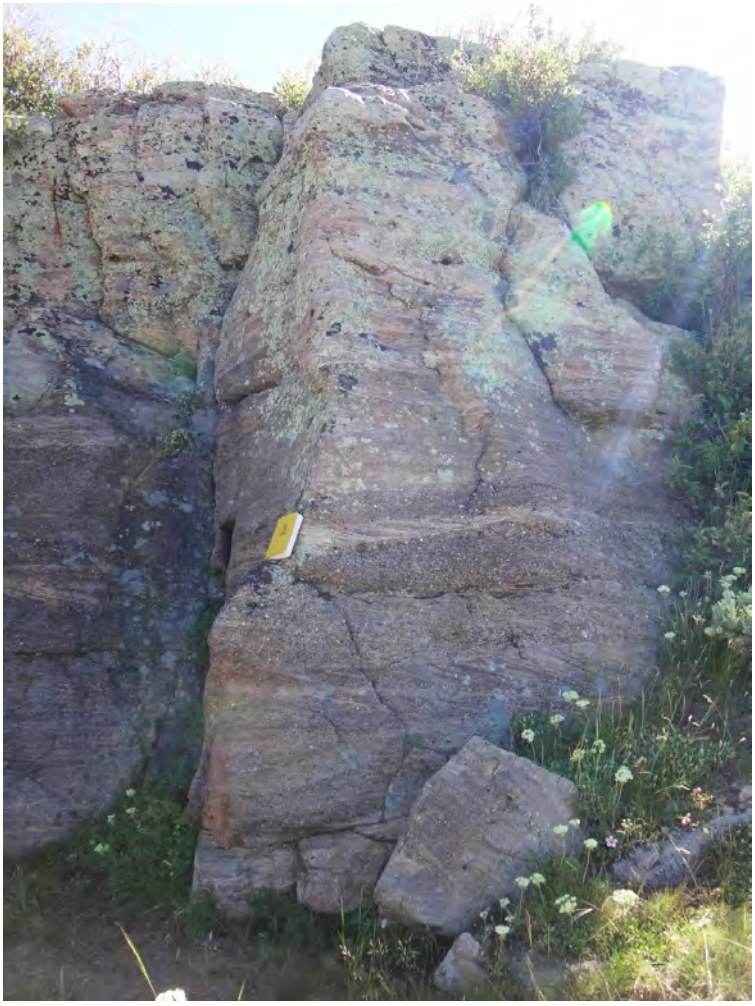

Figure 16. Chert conglomerate and cross-bedded sandstones at the base of the Cloverly Formation, T. 18 N., R. 89 W., sec. 26.

Figure 17. Lower Cretaceous and Jurassic formations in the Grove Creek drainage atop Miller Hill, T. 18 N., R. 89 W., sec. 26.

Jurassic

Morrison Formation (Jm): The Morrison Formation is composed of interbedded gray and varicolored siltstone with nodular freshwater limestone and thin sandstones (Love, 1953). Outcrops are limited to the Grove Creek drainage near the southeastern limit of the quadrangle, and exposure is generally poor. The Morrison Formation commonly forms slopes and is sparse in vegetation compared to the also poorly exposed Sundance Formation that are peppered with talus from overlying Cloverly Formation conglomerates and sandstones (fig. 17). The Morrison Formation is approximately 60 m (200 ft) thick in the Bridger Pass quadrangle.

The Morrison Formation is Kimmeridgian to Tithonian in age and was deposited in a continental environment (Picard, 1993). The contact between the Morrison Formation and the underlying Sundance Formation is conformable and indistinct. This contact is mapped where the variegated shale of the Morrison transitions to the greenish-gray of the uppermost Sundance Formation, and where the vegetation increases in density.

Sundance Formation (Js): The Sundance Formation in its uppermost parts consists of greenish-gray, glauconitic shale and sandstone, while the lower half of the formation is composed of pale red and gray siltstone and sandstone. Although the upper part is rich in marine fossils (Vine and Prichard, 1959), no fossils were observed in the Bridger Pass quadrangle where Sundance exposure is generally poor (fig. 17). Outcrops are limited to the Grove Creek drainage. The complete thickness of the Sundance Formation was not observed; its lowermost parts are covered by Miocene Browns Park Formation. Vine and Prichard (1959) estimate a thickness of 40 m (130 ft) in the vicinity of Miller Hill.

The Sundance Formation was deposited in the Late Jurassic during transgression and regression of the Sundance sea across the stable Wyoming shelf (Picard, 1993).

REFERENCES

Berry, D.W., 1960, Geology and ground-water resources of the Rawlins area, Carbon County, Wyoming: U.S. Geological Survey Water-Supply Paper 1458, 74 p., 1 pl., scale 1:63,360.

BLM, 2007, Environmental impact statement for the Atlantic Rim Natural Gas Field Development Project, Carbon County, Wyoming: Bureau of Land Management (BLM) Rawlins Field Office, 24 p.

Boggs, Sam, Jr., 2009, Petrology of sedimentary rocks: Cambridge University Press, 600 p.

Bircher, M.J., 2014, Depositional environment and reservoir characterization of the Paleocene Fort Union Formation, Washakie Basin, southwest Wyoming, USA: Colorado School of Mines, M.S. thesis, 173 p.

Buehner, J.H., 1936, Geology of an area north of the Sierra Madre, Carbon County, Wyoming: University of Wyoming, M.S. thesis, 37 p.

Buffler, R.T., 1967, The Browns Park Formation and its relationship to the late Tertiary geologic history of the Elkhead region, Northwestern Colorado – South Central Wyoming: University of California at Berkeley, Ph. D. dissertation, 175 p.

Carroll, C.J., Lynds, R.M., Ratigan, D.R., and Palkovic, M.J., 2015a, Report on the preliminary geologic maps of the Shamrock Hills and Rawlins Peak SW quadrangles, Carbon County, Wyoming: Wyoming State Geological Survey Open File Report 15-8, 33 p., 2 sheets, scale 1:24,000.

Carvajal-Ortiz, Humberto, and Gentzis, Thomas, 2015, Critical considerations when assessing hydrocarbon plays using Rock-Eval pyrolysis and organic petrology data—Data quality revisited: International Journal of Coal Geology, v. 152, p. 113–122.

Collier, A.J., 1925, Oil and gas in the Miller Hill-Lake Valley anticline, Carbon County, Wyoming: U.S. Geological Survey Press Release 483.

Curtis, J.B., Zumberge J.E., and Brown, S.W., 2013, Evaluation of Niobrara and Mowry Formation petroleum systems in the Powder River, Denver, and central basins of the Rocky Mountains, Colorado and Wyoming, USA: Houston Geological Society Bulletin, March 2013, p. 31–35.

Dames and Moore, 1978, Coal resource occurrence and coal development potential maps of the southwest quarter of the Bridger Pass 15-minute quadrangle, Carbon County, Wyoming: U.S. Geological Survey Open-File Report 78-649, 21 p., 23 pls., scale 1:24,000.

Davis, J.C., 1970, Petrology of Cretaceous Mowry Shale of Wyoming: AAPG Bulletin, 54, p. 487–502.

Dembicki, Harry, Jr., 2009, Three common source rock evaluation errors made by geologists during prospect or play appraisals: AAPG Bulletin, v. 93, no. 3, p. 341–356.

Finn, T.M., and Johnson, R.C., 2005, Niobrara total petroleum system in the southwestern Wyoming Province, chap. 6 *of* U.S. Geological Survey Southwestern Wyoming Province Assessment Team, comp., Petroleum systems and geologic assessment of oil and gas in the southwestern Wyoming Province, Wyoming, Colorado, and Utah: U.S. Geological Survey Digital Data Series 69-D, 27 p.

Gregory, R.W., Carnes, J.D., and Bagdonas, D.A., 2016, Zeolite resources in Wyoming: Wyoming State Geological Survey Report of Investigations 72, 65 p.

Gill, J.R., Merewether, E.A., and Cobban, W.A., 1970, Stratigraphy and nomenclature of some Upper Cretaceous and lower Tertiary rocks in south-central Wyoming: U.S. Geological Survey Professional Paper 667, 53 p.

Gomez-Veroiza, C.A., and Steel, R.J., 2010, Iles clastic wedge development and sediment partitioning within a 300-km fluvial to marine Campanian transect (3 my), Western Interior Seaway, southwestern Wyoming and northern Colorado: AAPG Bulletin, v. 94, no. 9, p. 1,349–1,377.

Haacke, J.E., Barclay, C.S.V., and Hettinger, R.D., 2016, Preliminary geologic mapping of Cretaceous and Tertiary formations in the eastern part of the Little Snake River coal field, Carbon County, Wyoming: U.S. Geological Survey Open-File Report 2016-1170, 9 p.

Harris, R.E., 2004, Industrial minerals and construction materials map of Wyoming: Wyoming State Geological Survey Map Series 47, scale 1:500,000.

Hettinger, R.D., Honey, J.G., Ellis, M.S., Barclay, C.S.V., and East, J.A., 2008, Geologic map of Upper Cretaceous and Tertiary strata and coal stratigraphy of the Paleocene Fort Union Formation, Rawlins-Little Snake River area, South-Central Wyoming: U.S. Geological Survey Scientific Investigations Map 3053, 3 sheets, scale 1:100,000.

King, J.K., and Harris, R.E., 2002, Natural zeolites in Wyoming: Wyoming State Geological Survey Open File Report 90-4, 51 p. (Revised.)

Kirschbaum, M.A., and Roberts, L.N.R., 2005, Stratigraphic framework of the Cretaceous Mowry Shale, Frontier Formation and adjacent units, southwestern Wyoming Province, Wyoming, Colorado, and Utah, chap. 15 *of* U.S. Geological Survey Southwestern Wyoming Province Assessment Team, comp., Petroleum systems and geologic assessment of oil and gas in the southwestern Wyoming Province, Wyoming, Colorado, and Utah: U.S. Geological Survey Digital Data Series 69-D, 21 p., 4 pls.

Landon, S.M., Longman, M.W., and Luneau, B.A., 2001, Hydrocarbon source rock potential of the Upper Cretaceous Niobrara Formation, Western Interior Seaway of the Rocky Mountain region: The Mountain Geologist, v. 28, no. 1, p. 1–18.

Larson, T.G., and Vieaux, D.G., 1951, Miller Hill area, Carbon County, Wyoming: Wyoming Geological Association Sixth Annual Field Conference Guidebook, p. 123–125.

Love, J.D., 1953, Preliminary report on uranium deposits in the Miller Hill area, Carbon County, Wyoming: U.S. Geological Survey Trace Elements Investigations Report 315, 46 p., 1 pl.

Luft, S.J., and Thoen, W.L., 1981, Measured sections of the Browns Park Formation (Miocene) in Moffat County, Colorado, 1980: U.S. Geological Survey Open-File Report 81-171, 35 p.

Luft, S.J., 1985, Airfall tuff in the Browns Park Formation northwestern Colorado and northeastern Utah: The Mountain Geologist, v. 22, no. 3, p. 110–127.

Luneau, Barbara, Longman, Mark, Kaufman, Peter, and Landon, Susan, 2011, Stratigraphy and petrophysical characteristics of the Niobrara Formation in the Denver Basin, Colorado and Wyoming: AAPG Rocky Mountain Section meeting, Cheyenne, Wyoming, USA, June 25-29, 2011.

Luo, Hongjun, and Nummedal, Dag, 2010, Late Cretaceous stratigraphy and tectonics across southwestern Wyoming: The Mountain Geologist, v. 47, no. 3, p. 91–116.

Lynds, R.N., and Lichtner, D.T., 2016, Stratigraphy and hydrocarbon potential of the Fort Union and Lance formations in the Great Divide and Washakie basins, South-Central Wyoming: Wyoming State Geological Survey Report of Investigations 73, 70 p., 2 pls.

Martinsen, O.J., 1994, Evolution of an incised-valley fill, the Pine Ridge Sandstone of southeastern Wyoming, U.S.A.—Systematic sedimentary response to relative sea-level change: Society for Sedimentary Geology (SEPM) Special Publication 51, p. 110–128.

McDonald, R.E., 1975, Structure, correlation, and depositional environments of the Tertiary Sand Wash and Washakie basins, Colorado and Wyoming, *in* Bolyard, D.W., editor, Rocky Mountain Association of Geologists symposium on deep drilling frontiers in the central Rocky Mountains, p. 100–103.

McLaughlin J.F., and Fruhwirth, Jeff, 2008, Preliminary geologic map of the Rawlins 30' x 60' quadrangle, Carbon and Sweetwater counties, southeastern Wyoming: Wyoming State Geological Survey Open File Report 08-4, scale 1:100,000.

Mellere, Donatella, and Steel, R.J., 1995, Facies architecture and sequentiality of nearshore and 'shelf' sandbodies; Haystack Mountains Formation, Wyoming, USA: Sedimentology, v. 42, p. 551–574.

Montagne, John, 1991, Cenozoic history of the Saratoga Valley area, Wyoming and Colorado: Rocky Mountain Geology, v. 29, p. 13–70.

Perman, R.C., 1987, Deltaic deposits of the Upper Cretaceous Dad Sandstone Member of the Lewis Shale, south-central Wyoming: Rocky Mountain Association of Geologists, v. 24, no. 1, p. 10–18.

Peters, K.E., 1986, Guidelines for evaluating petroleum source rock using programmed pyrolysis: AAPG Bulletin, v. 70, no. 3, p. 318–329.

Philp, R.P., and Galvez-Sinibaldi, A., 1991, Characterization of organic matter by various pyrolysis techniques, *in*. Merril, R.K., Foster, N.H., and Beaumont, E.D., editors, Source and migration processes and evaluations techniques, p. 107–112.

Picard, M.D., 1993, The early Mesozoic history of Wyoming, *in* Snoke, A.W., Steidtmann, J.R., and Roberts, S.M., editors, Geology of Wyoming: Geological Survey of Wyoming Memoir No. 5., p. 210–248.

Pyles, D.R., and Slatt, R.M., 2000, A high-frequency sequence stratigraphic framework for shallow through deep-water deposits of the Lewis Shale and Fox Hills Sandstone, Great Divide and Washakie basins, Wyoming, *in* Weimer, Paul, Slatt, R.M., Coleman, Jim, Rosen, Norman, Nelson, Hans, Bouma, A.H., Styzen, M.J., and Lawrence, D.T., editors, Deep-water reservoirs of the world: Gulf Coast Section Society of Economic Paleontologists and Mineralogists Foundation, 20th annual Bob F. Perkins Research Conference, Houston, Texas, December 3-6, 2000, p. 836–861.

Quillinan, S.A., Worman, B.N., and Rodgers, J.R., 2009, Coalbed natural gas activity in the Atlantic Rim area, Carbon County, Wyoming: Wyoming State Geological Survey Open File Report 09-7, scale 1:100,000.

Roehler, H.W., 1990, Stratigraphy of the Mesaverde Group in the central and eastern Greater Green River Basin, Wyoming, Colorado, and Utah: U.S. Geological Survey Professional Paper 1508, 52 p., 2 pls.

Rudolph, K.W., Devlin, W.J., and Crabaugh, J.P., 2015, Upper Cretaceous sequence stratigraphy of the Rock Springs Uplift, Wyoming: Rocky Mountain Geology, v. 52, p. 13–157.

Sonnenberg, S.A., 2012, The Niobrara petroleum system, Rocky Mountain region: Tulsa Geological Society dinner meeting, Tulsa, Oklahoma, January 3, 2012.

Steidtmann, J.R., 1993, The Cretaceous foreland basin and its sedimentary record, *in* Snoke, A.W., Steidtmann, J.R., and Roberts, S.M., editors, Geology of Wyoming: Geological Survey of Wyoming Memoir No. 5, p. 250–271.

Vincelette, R.R., and Foster, N.H., 1992, Fractured Niobrara of northwestern Colorado, *in* Schmoker, J.W., Coalson, E.B., and Brown, C.A., editors, Geological studies relevant to horizontal drilling—Examples from western North America: Rocky Mountain Association of Geologists Guidebook, p. 227–239.

Vine, J.D., and Prichard, G.E., 1959, Geology and uranium occurrences in the Miller Hill area, Carbon County, Wyoming: U.S. Geological Survey Bulletin 1074-F, p. 201–239.

Weitz, J.L., and Love, J.D., 1953, Geologic map of Carbon County, Wyoming: Geological Survey of Wyoming.

WOGCC, 2017, Wyoming Oil and Gas Conservation Commission, accessed July 2017, at http://wogcc.state.wy.us/.

Appendix 1

APPENDIX 1: PRELIMINARY PETROGRAPHIC ANALYSIS

Blue epoxy-impregnated thin sections were created by Wagner Petrographic, Inc. for 13 sandstone samples from within the Haystack Mountains and Almond formations. Related Mesaverde sandstones are targeted in the nearby Washakie Basin as both conventional and unconventional reservoirs.

Herein, the authors of this report present a preliminary—and qualitative—assessment of the composition (mineralogy, diagenesis, and porosity) and texture (Wentworth grain size classification, sorting, sphericity, and roundness) of each thin section. Additional resources on petrographic analysis of sedimentary rocks may be found in Boggs (2009) and numerous other sources.

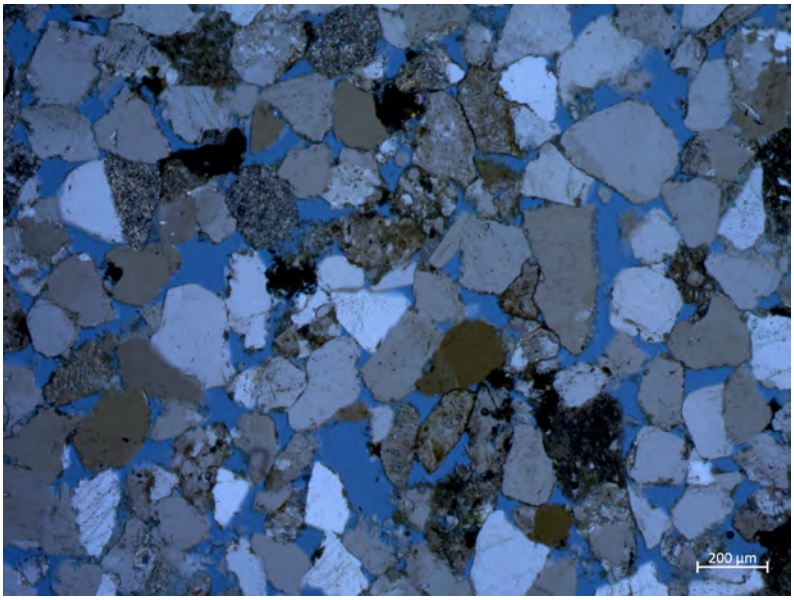

Figure A1–1. Photomicrograph (XPL) of sample 20170607JC-1A, a sandstone from the upper portion of the Steele Shale (Ks). This sandstone is a litharenite composed primarily of monocrystalline quartz and lithic fragments, with minor components of seriticized sodium plagioclase, isotropic (opaque) minerals, and considerable primary porosity. There is minimal fine-grained matrix. During diagenesis, minor dissolution of lithic fragments occurred, as well as moderate compaction and suturing of quartz grains. Grains are fine-grained sand, moderately well sorted, and generally subangular to subrounded, with low to moderate sphericity.

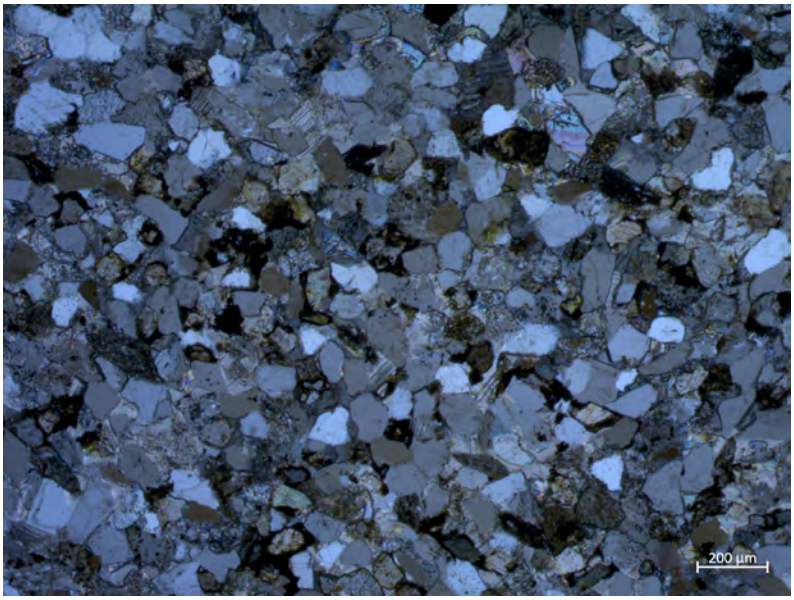

Figure A1–2. Photomicrograph (XPL) of sample 20170607JC-2A from the Tapers Ranch Sandstone (Khmt), the lowermost sandstone of the Haystack Mountains Formation (Khm). This sandstone is a litharenite composed primarily of quartz and lithic fragments, with minor amounts of sodium plagioclase, opaque minerals, and micas (seritcite and muscovite), with generally low porosity. During diagenesis ,there was considerable compaction and fusion of quartz grains. Alteration products from the dissolution of lithic fragments and plagioclase minerals occupy much of the sample's primary porosity. Most of the effective porosity is secondary and resulted from further dissolution of mineral grains. Grains are very fine grained sand, moderately well sorted, and subangular, with low, occasionally elongate, sphericity.

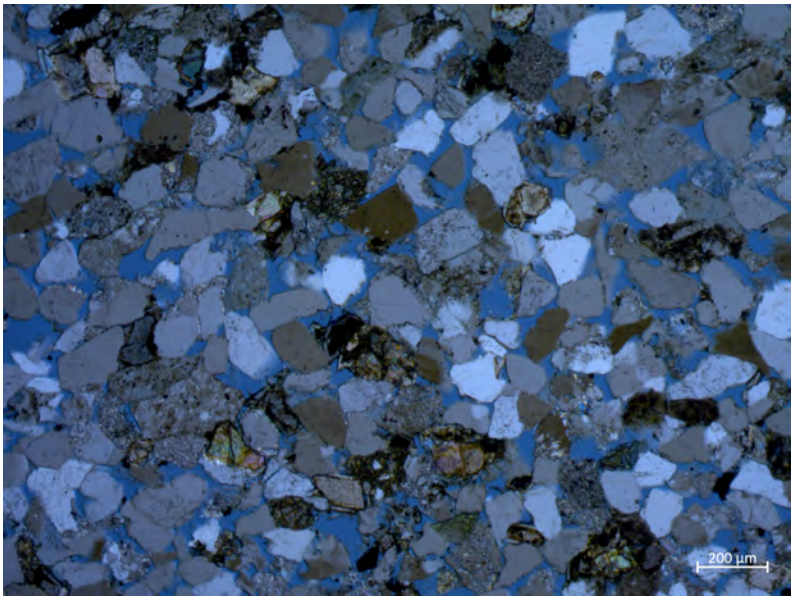

Figure A1–3. Photomicrograph (XPL) of sample 20170607JC-3A from the O'Brien Spring Sandstone (Khmo), a sandstone within the Haystack Mountains Formation (Khm). This sandstone is a litharenite composed primarily of quartz and lithic fragments, with minor amounts of sodium plagioclase, opaque minerals, and micas (seritcite and muscovite), with moderate porosity. During diagenesis, there was moderate compaction and fusion of quartz grains and dissolution of lithic fragments. Most of the effective porosity is primary, with some secondary porosity from dissolution. Grains are very fine to fine grained sand, moderately sorted, and angular to subrounded, with elongate to low sphericity.

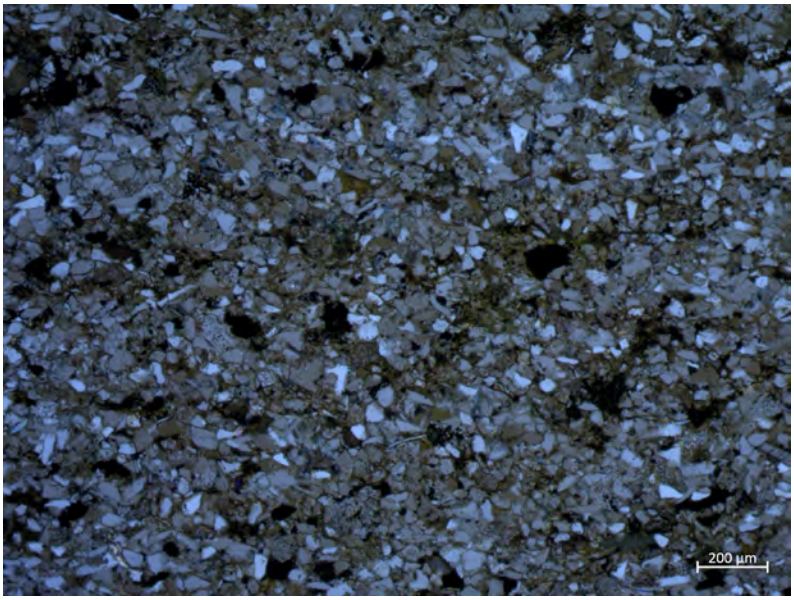

Figure A1–4. Photomicrograph (XPL) of sample 20170607JC-4B from the Seminoe-2 sandstone (Khms), a sandstone within the Haystack Mountains Formation (Khm). This sandstone is a sublitharenite composed primarily of quartz, with minor amounts of lithic fragments, opaque minerals, sodium plagioclase, and micas, with generally low porosity. During diagenesis, there was moderate dissolution of mineral grains and filling of pore spaces with fine-grained matrix material. Grains are medium silt to very fine grained sand, well sorted, and subangular, with low sphericity. Elongate grains are moderately imbricated.

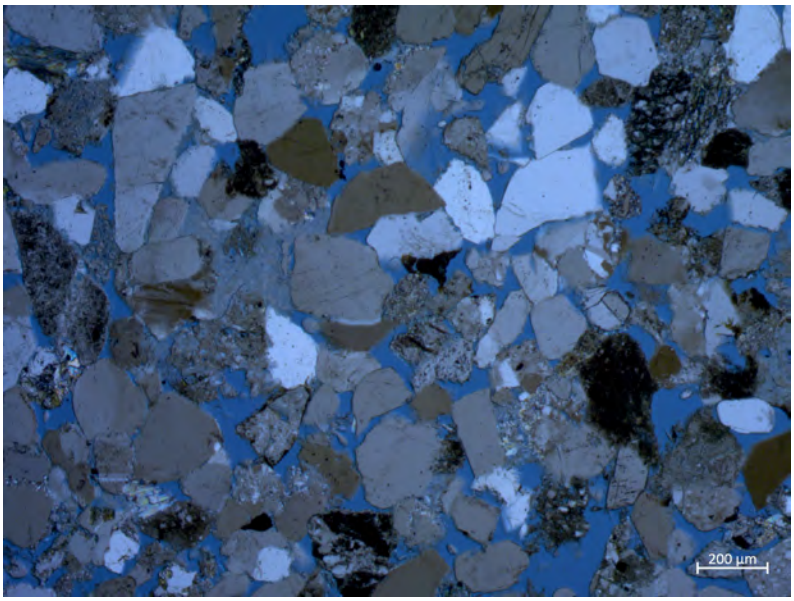

Figure A1–5. Photomicrograph (XPL) of sample 20170607JC-4C from the Seminoe-3 sandstone (Khms), a sandstone within the Haystack Mountains Formation (Khm). This sandstone is a litharenite composed primarily of quartz and lithic fragments, with minor amounts of opaque minerals and micas, with considerable porosity. During diagenesis, there was moderate compaction, resulting in fracturing of some quartz grains, as well as minor dissolution of lithic fragments. Most of the effective porosity is primary, with some secondary porosity from dissolution. Grains are fine grained sand, moderately sorted, and angular to subrounded, with low sphericity.

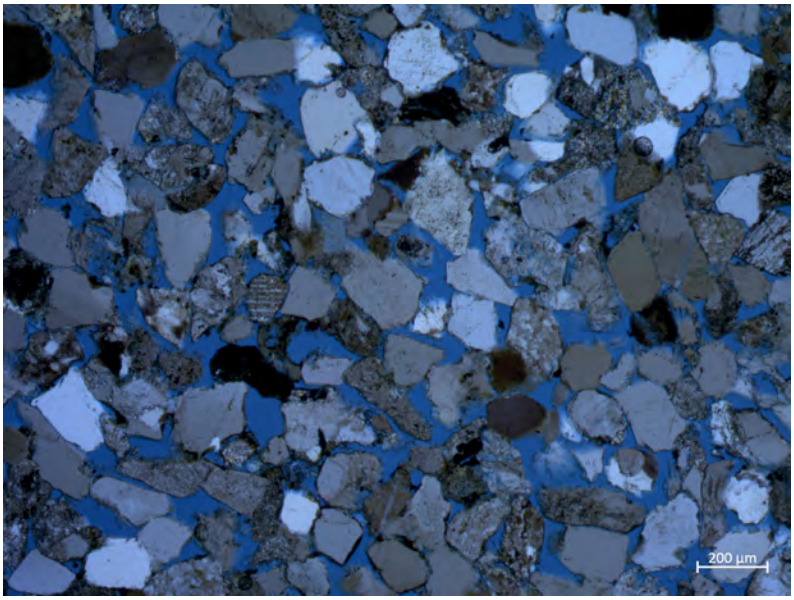

Figure A1–6. Photomicrograph (XPL) of sample 20170607JC-4D from the Seminoe-4 sandstone (Khms), a sandstone within the Haystack Mountains Formation (Khm). This sandstone is a litharenite composed primarily of quartz and lithic fragments, with minor amounts of opaque minerals and micas, including glacuonite, with considerable porosity. During diagenesis, there was moderate compaction and fusion of quartz grains, as well as moderate dissolution of lithic fragments. Most of the effective porosity is primary, with some secondary porosity from dissolution. Grains are fine grained sand, moderately sorted, and angular to subangular, with elongate to low sphericity.

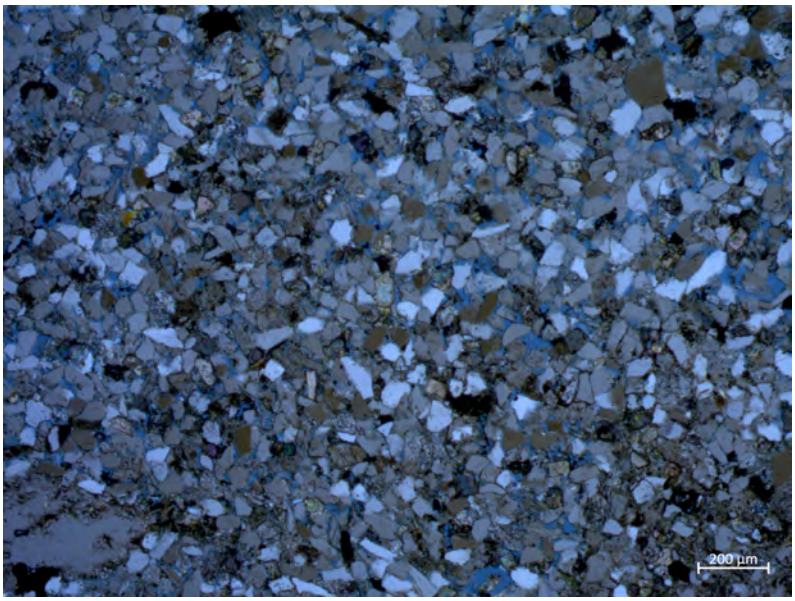

Figure A1–7. Photomicrograph (XPL) of sample 20170607JC-5A from near the bottom of the Hatfield-1 sandstone (Khmh), a sandstone within the Haystack Mountains Formation (Khm). This sandstone is a sublitharenite composed primarily of quartz and lithic fragments, with minor amounts of opaque minerals and micas, with low to moderate porosity. During diagenesis, there was minor compaction, as well as considerable dissolution of lithic fragments. Most of the effective porosity is primary. Dissolution served to both create secondary porosity and fill primary pore spaces. Grains are coarse silt to fine grained sand, moderately sorted, and subangular, with elongate to low sphericity.

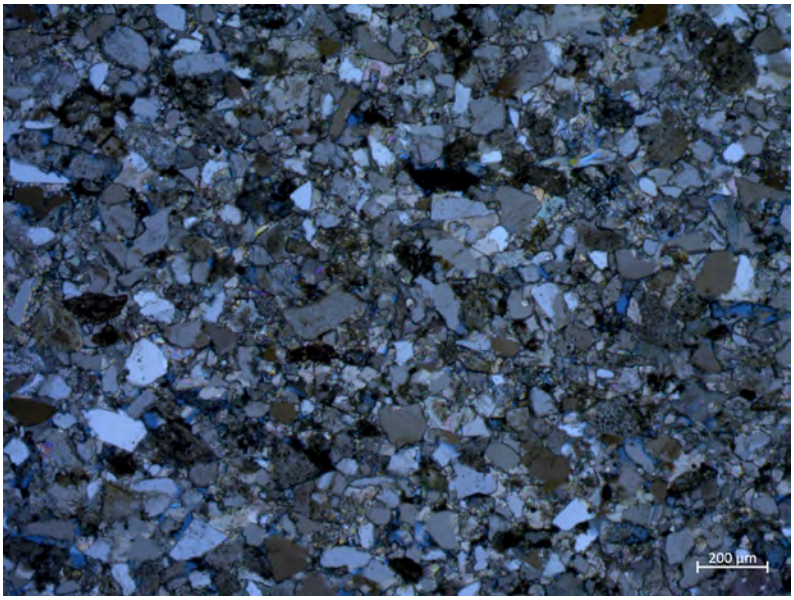

Figure A1–8. Photomicrograph (XPL) of sample 20170607JC-5B from near the top of the Hatfield-1 sandstone (Khmh), a sandstone within the Haystack Mountains Formation (Khm). This sandstone is a litharenite composed primarily of quartz and lithic fragments, with minor amounts of opaque minerals and micas and rare plagioclase, with low porosity. During diagenesis, there was moderate compaction, resulting in fracturing and fusion of quartz grains, as well as considerable dissolution of lithic fragments. Alteration products from mineral dissolution resulted in the elimination of much of the primary porosity. Grains are coarse silt to fine grained sand, poorly to moderately sorted, and angular to subangular, with elongate to low sphericity.

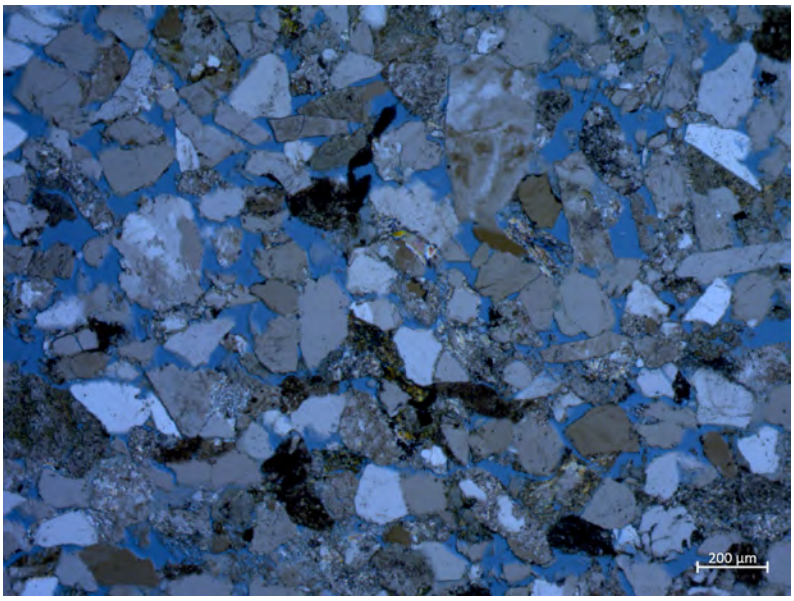

Figure A1–9. Photomicrograph (XPL) of sample 20170607JC-6A from the Hatfield-2 sandstone (Khmh), a sandstone within the Haystack Mountains Formation (Khm). This sandstone is a litharenite composed primarily of quartz and lithic fragments, with minor amounts of opaque minerals, with considerable porosity. During diagenesis, there was minor dissolution of lithic fragments. Much of the effective porosity is primary, with the addition of minor secondary porosity resulting from dissolution. Grains are fine grained sand, moderately sorted, and subangular, with elongate to low sphericity.

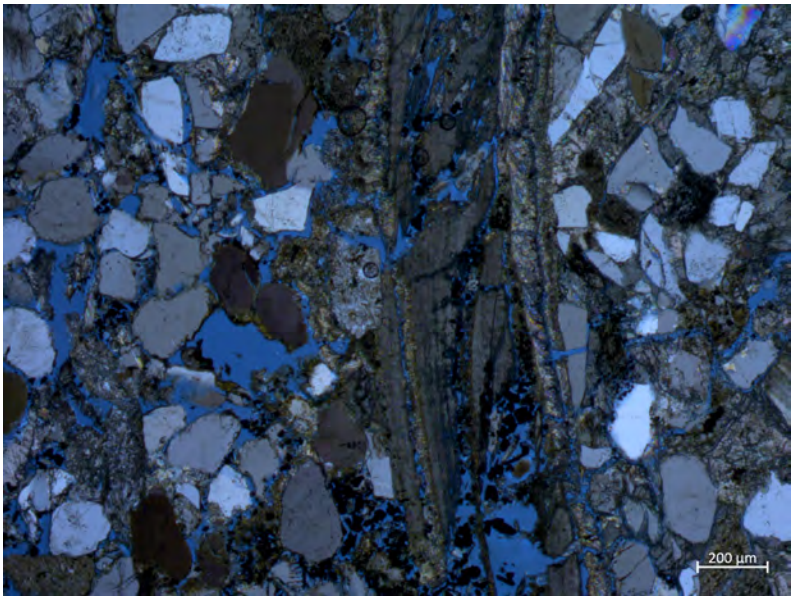

Figure A1–10. Photomicrograph (XPL) of sample 20170607JC-6B from the top of the Hatfield-2 sandstone (Khmh), a sandstone within the Haystack Mountains Formation (Khm). This sandstone is a sublitharenite composed primarily of quartz, fossil shell fragments, and lithic fragments with minor amounts of opaque minerals and sodium plagioclase, and low to moderate porosity. During diagenesis, there was moderate dissolution of lithic and fossil fragments and the precipitation of secondary calcite cement. Much of the effective porosity is secondary, resulting from dissolution. Grains are fine to medium grained sand, poorly to moderately sorted, and subangular, with elongate to low sphericity.

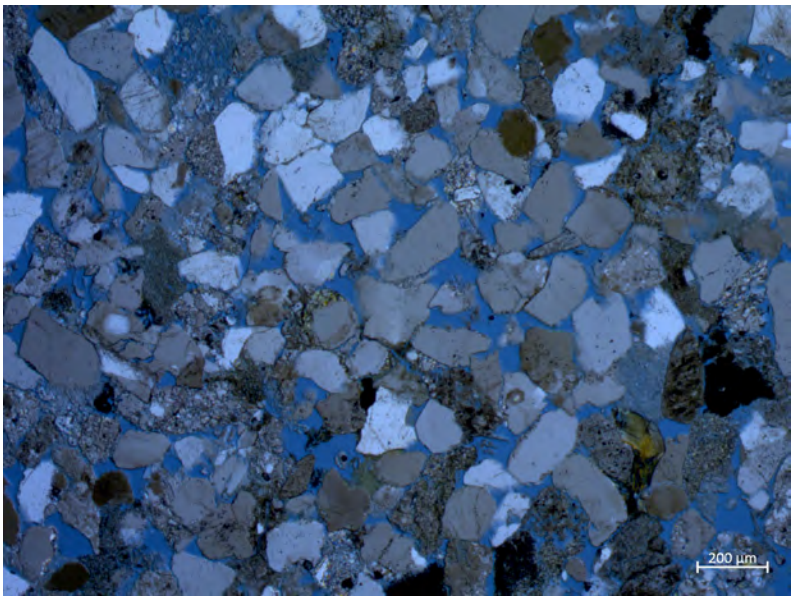

Figure A1–11. Photomicrograph (XPL) of sample 20170607JC-7A from an unnamed sandstone in the uppermost portion of the Haystack Mountains Formation (Khm). This sandstone is a litharenite composed primarily of quartz and lithic fragments, with minor amounts of opaque minerals, micas, and calcite, and moderate porosity. During diagenesis, there was minor dissolution of lithic fragments. Much of the effective porosity is primary, with the addition of minor secondary porosity resulting from dissolution. Grains are fine grained sand, moderately sorted, and angular to subangular, with low sphericity.

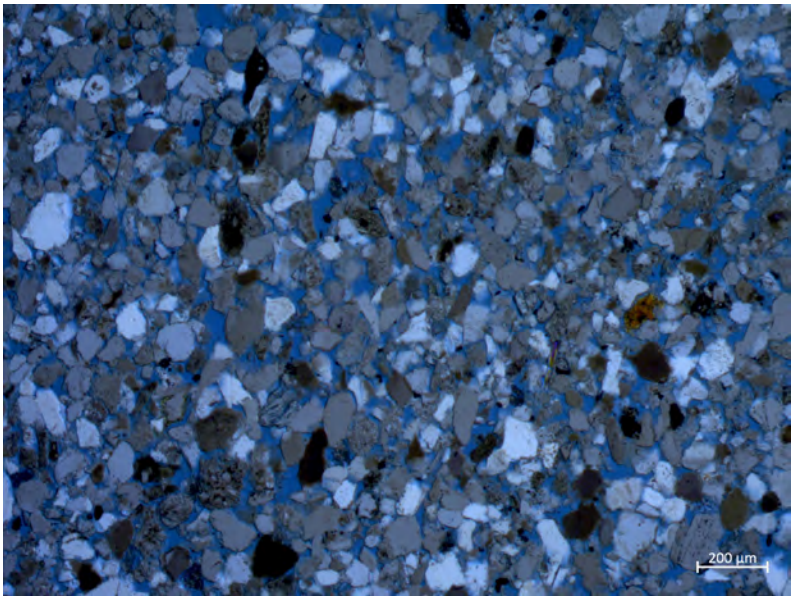

Figure A1–12. Photomicrograph (XPL) of sample 20170608JC-1B from a sandstone within the central coal-bearing portion of the Almond Formation (Kal). This sandstone is a sublitharenite composed primarily of quartz and lithic fragments, with minor amounts of opaque minerals, and moderate porosity. During diagenesis, there was minor compaction and fusion of grains. Much of the effective porosity is primary. Grains are very fine grained sand, moderately sorted, and subangular, with elongate to medium sphericity.

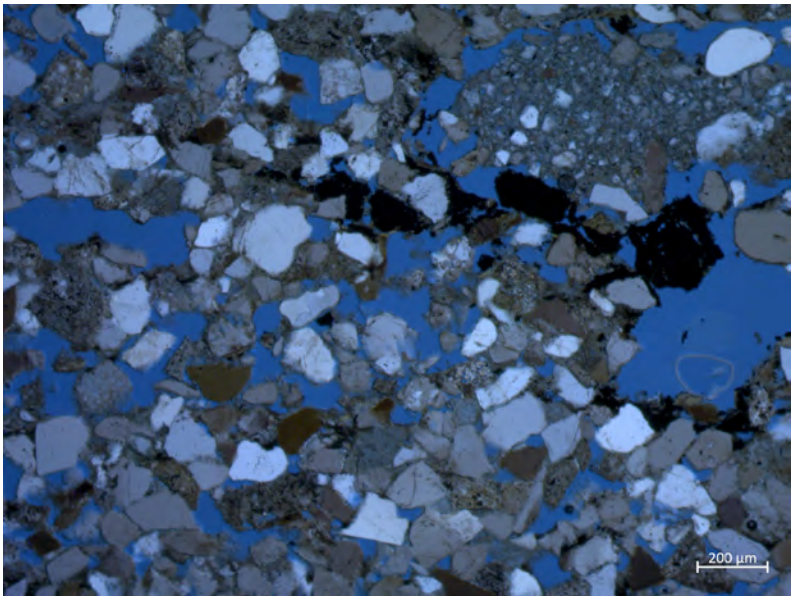

Figure A1–13. Photomicrograph (XPL) of sample 20170608JC-3A from a sandstone near the bottom of the Almond Formation (Kal). This sandstone is a sublitharenite composed primarily of quartz and lithic fragments, with minor amounts of opaque minerals and micas, including glacuonite, with moderate porosity. Rare rip-up clasts, greater than 3 mm in diameter, of fine-grained material are present. During diagenesis, there was minor growth of fine-grained clays and mica rinds around grains. Much of the effective porosity is primary, with the addition of minor secondary porosity resulting from dissolution. The sandstone is poorly cemented, and grains feature minor imbrication. Grains are very fine to fine-grained sand, poorly to moderately sorted, and subangular, with elongate to low sphericity.

Appendix 2

APPENDIX 2: COAL QUALITY ANALYSIS

Five coal samples were assessed using short proximate (short prox) and ultimate proximate (ultimate prox) methods, and for trace metals and vitrinite reflectance, at Wyoming Analytical Laboratories (WAL). Together, short prox, ultimate prox, and trace metals analyses provide data useful for evaluating a coal's potential as an energy resource. Vitrinite reflectance can be used to assess the thermal maturity of a coal bed or hydrocarbon source rock. Further information on gathering and evaluating coal quality data may be found in:

Palmer, C.A., Oman, C.L., Park, A.J., and Luppens, J.A., 2015, The U.S. Geological Survey coal quality (COALQUAL) database version 3.0: U.S. Geological Survey Data Series 975, 43 p. with appendixes. Herein, the authors of this report present the data without interpretation.

Each analyzed sample was sourced from a coal bed in the Almond Formation (Kal) of the Mesaverde Group except for Sample 20170531JC-1A, which was collected from the uppermost shales of the Haystack Mountains Formation (Khm). Data are presented on pages 34–38 of this report.

Coal quality and thermal maturity data for ***Sample 20170531JC-1A***, a coal from the uppermost part of the Haystack Mountains Formation (Khm).

Proximate Analysis

Component	As received (wt%)	Moisture free (wt%)	Moisture & ash free (wt%)
Moisture	9.99	-	-
Ash	6.85	7.61	-
Volatile Matter	40.41	44.90	45.59
Fixed Carbon	42.75	47.49	51.41
Total	**100.00**	**100.00**	**100.00**

Ultimate Analysis

Component	As received (wt%)	Moisture free (wt%)	Moisture & ash free (wt%)
Moisture	9.99	-	-
Ash	6.85	7.61	-
Carbon	57.30	63.66	68.90
Hydrogen	3.38	3.76	4.07
Nitrogen	0.96	1.07	1.15
Sulfur	0.49	0.54	0.59
Oxygen	21.03	23.36	25.29
Total	**100.00**	**100.00**	**100.00**

Heating Value

As received (Btu/lb)	Moisture free (Btu/lb)	Moisture & ash free (Btu/lb)
9,559	10,620	11,495

Trace Elements	Concentration (mg/kg)
Beryllium	0.333
Vanadium	12.3
Chromium	4.62
Manganese	9.67
Cobalt	1.29
Nickel	9.13
Copper	8.45
Zinc	10.6
Arsenic	0.578
Molybdenum	2.98
Cadmium	0.193
Antimony	0.119

Vitrinite Reflectance

Romax	σRomax	Rorandom	σRorandom
0.43	0.05	0.38	0.05

Coal quality and thermal maturity data for ***Sample 20170531JC-2A***, a coal from the Almond Formation (Kal) in the northern part of the quadrangle.

Proximate Analysis

Component	As received (wt%)	Moisture free (wt%)	Moisture & ash free (wt%)
Moisture	10.37	-	-
Ash	25.90	28.90	-
Volatile Matter	32.07	35.78	50.32
Fixed Carbon	31.66	35.32	49.68
Total	**100.00**	**100.00**	**100.00**

Ultimate Analysis

Component	As received (wt%)	Moisture free (wt%)	Moisture & ash free (wt%)
Moisture	10.37	-	-
Ash	25.90	28.90	-
Carbon	39.62	44.20	62.17
Hydrogen	2.32	2.59	3.64
Nitrogen	0.45	0.50	0.71
Sulfur	0.32	0.36	0.50
Oxygen	21.02	23.45	32.98
Total	**100.00**	**100.00**	**100.00**

Heating Value

As received (Btu/lb)	Moisture free (Btu/lb)	Moisture & ash free (Btu/lb)
6,262	6,987	9,826

Trace Elements	Concentration (mg/kg)
Beryllium	2.21
Vanadium	28.7
Chromium	9.52
Manganese	5.48
Cobalt	12.0
Nickel	40.0
Copper	13.1
Zinc	80.3
Arsenic	1.30
Molybdenum	4.36
Cadmium	1.30
Antimony	0.947

Vitrinite Reflectance

Romax	σRomax	Rorandom	σRorandom
0.46	0.04	0.39	0.04

Coal quality and thermal maturity data for ***Sample 20170531JC-3A***, a coal from the Almond Formation (Kal) in the northern part of the quadrangle.

Proximate Analysis

Component	As received (wt%)	Moisture free (wt%)	Moisture & ash free (wt%)
Moisture	10.30	-	-
Ash	13.19	14.70	-
Volatile Matter	36.59	40.79	47.82
Fixed Carbon	39.92	44.50	52.18
Total	**100.00**	**100.00**	**100.00**

Ultimate Analysis

Component	As received (wt%)	Moisture free (wt%)	Moisture & ash free (wt%)
Moisture	10.30	-	-
Ash	13.19	14.70	-
Carbon	50.22	55.99	65.64
Hydrogen	2.80	3.12	3.66
Nitrogen	0.61	0.68	0.80
Sulfur	0.36	0.40	0.47
Oxygen	22.52	25.11	29.44
Total	**100.00**	**100.00**	**100.00**

Heating Value

As received (Btu/lb)	Moisture free (Btu/lb)	Moisture & ash free (Btu/lb)
8,188	9,128	10,702

Trace Elements	Concentration (mg/kg)
Beryllium	1.63
Vanadium	20.4
Chromium	10.9
Manganese	62.9
Cobalt	8.75
Nickel	5.82
Copper	9.51
Zinc	41.7
Arsenic	0.810
Molybdenum	4.28
Cadmium	0.406
Antimony	0.373

Vitrinite Reflectance

Romax	σRomax	Rorandom	σRorandom
0.50	0.03	0.40	0.07

Coal quality and thermal maturity data for ***Sample 20170608JC-1A***, a coal from the Almond Formation (Kal) in the southwestern part of the quadrangle.

Proximate Analysis

Component	As received (wt%)	Moisture free (wt%)	Moisture & ash free (wt%)
Moisture	12.27	-	-
Ash	6.40	7.30	-
Volatile Matter	38.75	44.17	47.65
Fixed Carbon	42.58	48.54	52.35
Total	**100.00**	**100.00**	**100.00**

Ultimate Analysis

Component	As received (wt%)	Moisture free (wt%)	Moisture & ash free (wt%)
Moisture	12.27	-	-
Ash	6.40	7.30	-
Carbon	54.29	61.88	66.75
Hydrogen	2.97	3.38	3.65
Nitrogen	0.80	0.91	0.98
Sulfur	0.16	0.18	0.20
Oxygen	23.11	26.35	28.42
Total	**100.00**	**100.00**	**100.00**

Heating Value

As received (Btu/lb)	Moisture free (Btu/lb)	Moisture & ash free (Btu/lb)
8,833	10,068	10,861

Trace Elements	Concentration (mg/kg)
Beryllium	0.134
Vanadium	5.21
Chromium	2.94
Manganese	6.97
Cobalt	1.10
Nickel	3.06
Copper	5.01
Zinc	9.05
Arsenic	0.375
Molybdenum	0.781
Cadmium	0.115
Antimony	0.104

Vitrinite Reflectance

Romax	σRomax	Rorandom	σRorandom
0.47	0.05	0.41	0.04

Coal quality and thermal maturity data for ***Sample 20170608JC-2A***, a coal from the Almond Formation (Kal) in the west-central part of the quadrangle.

Proximate Analysis

Component	As received (wt%)	Moisture free (wt%)	Moisture & ash free (wt%)
Moisture	12.19	-	-
Ash	5.84	6.65	-
Volatile Matter	40.30	45.89	49.16
Fixed Carbon	41.67	47.45	50.84
Total	**100.00**	**100.00**	**100.00**

Ultimate Analysis

Component	As received (wt%)	Moisture free (wt%)	Moisture & ash free (wt%)
Moisture	12.19	-	-
Ash	5.84	6.65	-
Carbon	53.58	61.02	65.37
Hydrogen	2.84	3.23	3.46
Nitrogen	0.74	0.84	0.90
Sulfur	0.38	0.43	0.46
Oxygen	24.43	27.83	29.81
Total	**100.00**	**100.00**	**100.00**

Heating Value

As received (Btu/lb)	Moisture free (Btu/lb)	Moisture & ash free (Btu/lb)
8,564	9,753	10,448

Trace Elements	Concentration (mg/kg)
Beryllium	0.315
Vanadium	6.98
Chromium	3.51
Manganese	5.11
Cobalt	1.30
Nickel	5.52
Copper	8.85
Zinc	10.3
Arsenic	0.304
Molybdenum	2.01
Cadmium	0.178
Antimony	0.125

Vitrinite Reflectance

Romax	σRomax	Rorandom	σRorandom
0.49	0.05	0.41	0.06

Appendix 3

APPENDIX 3: SOURCE ROCK ANALYSIS

Three rock samples were analyzed with HAWK programmed pyrolysis and an LECO carbon analyzer at ALS Oil & Gas Laboratories. Programmed pyrolysis measures the hydrocarbon generation potential and thermal maturity of source rocks, whereas the carbon analyzer supplements pyrolysis data with a direct measurement total organic carbon (TOC). From these data, one may examine a source rock's free hydrocarbon content (S1 pyrolysis peak), generatable hydrocarbon content (S2 pyrolysis peak), generatable Co_2 (S3 pyrolysis peak), and kerogen type (determined from a Van Krevelen diagram), as well as other quantities useful for evaluating hydrocarbon generation potential. Philp and Galvez-Sinibaldi (1991), Dembick (2009), and Carvajal and Gentzis (2015), among others, summarize common methods and considerations for evaluating pyrolysis and TOC data. Herein, the authors of this report present the data and provide a brief, preliminary interpretation.

Each analyzed sample was sourced from one of three calcareous benches in the Niobrara Formation (Buck Peak, Tow Creek, and Wolf Mountain benches, from youngest to oldest; Vincelette and Foster, 1992). Data are presented in Table A3-1. Based on classic guidelines given by Peters (1986), the Tow Creek bench sample has the highest hydrocarbon source rock potential; in particular, the Tow Creek bench has "fair" to "very good" generation potential, whereas both the Buck Peak and Wolf Mountain benches have "poor" to "good" generation potential. All three samples exhibit Type-II, oil-prone kerogen. All also are within the thermal maturity window for oil generation.

These data are generally comparable with those from other studies in the region (Vincelette and Foster, 1992; Landon and others, 2001; Finn and Johnson, 2005). However, the Tow Creek bench sample in this study has TOC, S2, and hydrogen index values greater than those expected for south-central Wyoming, with a source rock richness more similar to that of the Niobrara Formation in the Denver-Julesburg Basin to the east (Luneau and others, 2011; Sonnenberg, 2012; Curtis and others, 2013).

It should be noted that the source rock analysis conducted as part of this study was extremely limited in both quantity and breadth, and more comprehensive analysis would be needed to assess whether the data are not only reproducible but also indicative of a regional, rather than local, trend.

Table A3–1. An LECO carbon analyzer TOC and measured and derived parameters from HAWK pyrolysis and for three Niobrara source rock samples.

Sample Name	Location in Section	Latitude (WGS84)	Longitude (WGS84)	Total Organic Carbon - TOC (wt%)	Free Hydrocarbons - S1 (mg HC / g rk)	Generatable Hydrocarbons - S2 (mg HC / g rk)	Temp of Peak S2 - Tmax (°C)	Generatable CO_2 - S3 (mg CO2 / g rk)
20170622DL-1A	Buck Peak bench (Knb)	41.531	-107.406	1.244	0.04	1.58	437	1.04
20170706DL-1A	Tow Creek bench (Knt)	41.500	-107.444	2.519	0.31	6.59	432	0.61
20170622DL-3A	Wolf Mountain bench (Knw)	41.504	-107.426	1.709	0.18	3.3	438	0.65